Exploratory data analysis and non-parametric methods for point pattern analysis for fluorescent microscopic images and digital X-ray detectors

Julia Brettschneider

University of Warwick, 14.2.2022

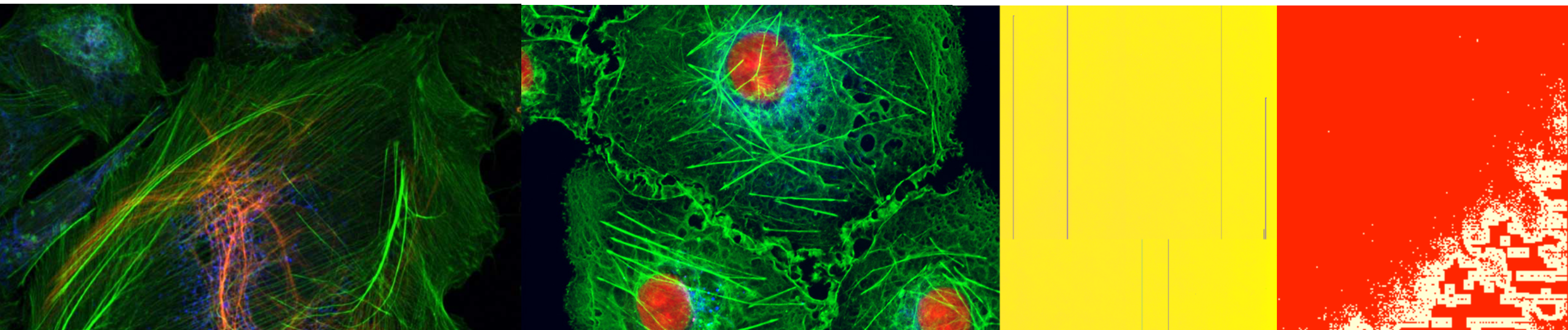

https://warwick.ac.uk/fac/sci/statistics/staff/academic-research/brettschneider/

Applied statistician/data scientists

Collaborators: engineers, life scientists, clinicians

Domains: genomics, microscopy, cancer, screening, finance, OR

Methodological topics: data quality, spatial statistics, decision theory, concepts of probability and risk

Short biography

- Reader (since 2021), Associate Professor (2010-2021), Assistant Professor (2007-2010), Dept of Statistics, University of **Warwick, UK**
- **Turing fellow** since 2017
- Assistant Professor, Dept of Math/Stats & Dept of Community Health/Epidemiology & Cancer Research Institute, **Queen's University, CN**
- Visiting Assistant Professor and Research Statistician, Dept of Statistics at **University of California at Berkeley, USA**
- Postdoctoral fellow in Computational Biology at **Eurandom, NL**
- PhD (2001) in Mathematics, thesis supervisor Prof. H. Föllmer, **Humboldt Uni. Berlin, D**
- Masters in Mathematics (with Computer Sciences and Psychology), thesis supervisor Prof. H. Föllmer, **University Bonn, D**

This was my first slide at my Warwick job talk in 2007!

My path

Research in applied statistics:

methods for statistical analysis of high-dim. molecular measurements (pre-processing, QA)

Postdoc period/now

Research in probability/ theoret. statistics:

measure valued diffusion proc. & quasilinear pde,
large deviations for random fields

Master's
PhD

now

Learning genomics:

molecular biology basics, genetics, genomics,
high-throughput measurement technology

"Wege entstehen indem man sie geht."
(Paths are created by walking them.)

Franz Kafka

Preamble: Applied mathematics as bridge

> *"The **instrument that mediates between theory and practice**, between thought and observation, is mathematics; it builds the **connecting bridge** and makes it stronger and stronger. Thus it happens that our entire present-day culture, insofar as it rests on intellectual insight into and harnessing of nature, is founded on mathematics."*
>
> David Hilbert

In Königsberg on 8 September 1930, David Hilbert addressed the yearly meeting of the Society of German Natural Scientists and Physicians (Gesellschaft der Deutschen Naturforscher und Ärzte).
Full text of the speech in English and German at url below, including audio file:

http://math.sfsu.edu/smith/Documents/HilbertRadio/HilbertRadio.pdf

Outline

Microscopy

… using images to quantify spatial abundance of protein

Microtubules formation during mitosis

… probabilistic point patterns

… statistical summaries and tests

… case study: microtubules during mitosis with TACC3 overexpression

Dead pixel formations on digital X-ray detectors

Dependencies between bulk movement patterns

… colocalisation

… earth movers distance and comparison statistics

… tests for a variety of hypotheses

… simulations and real data applications

Microscopy to observe quantifying spatial abundance of proteins

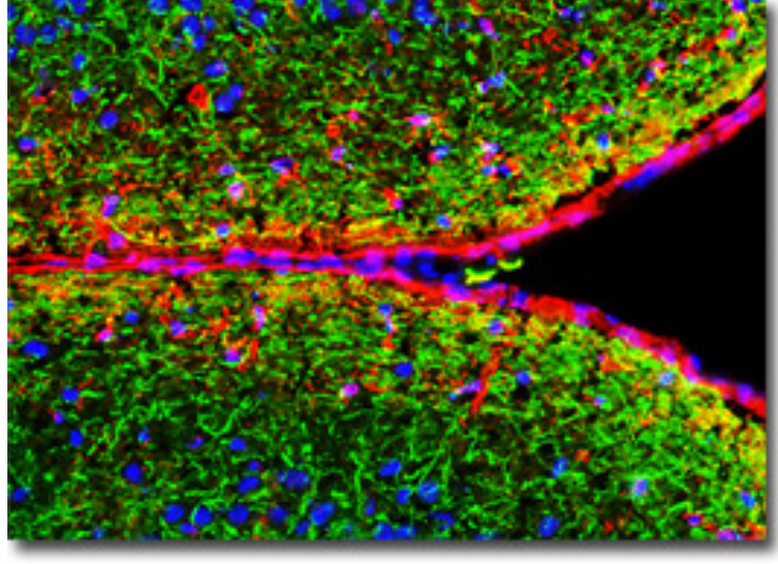

Confocal fluorescent laster microscopy (live cells)

Electron microscopy (dead cells, higher resolution)

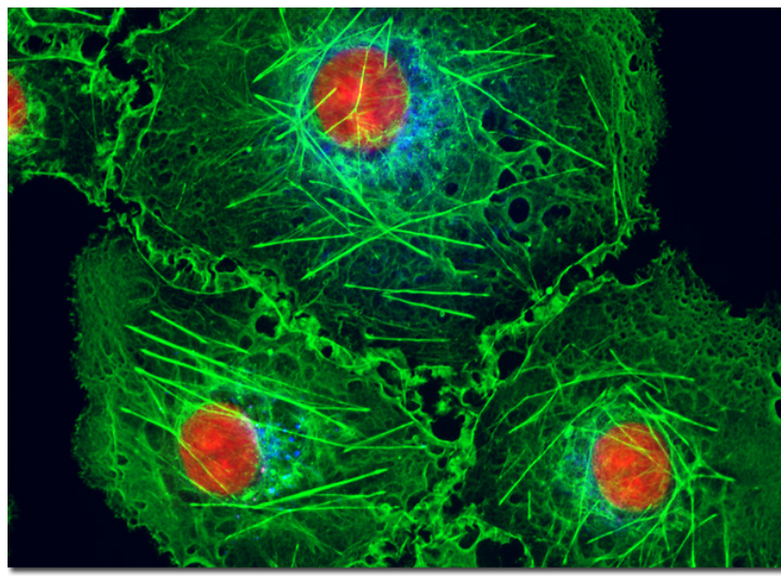

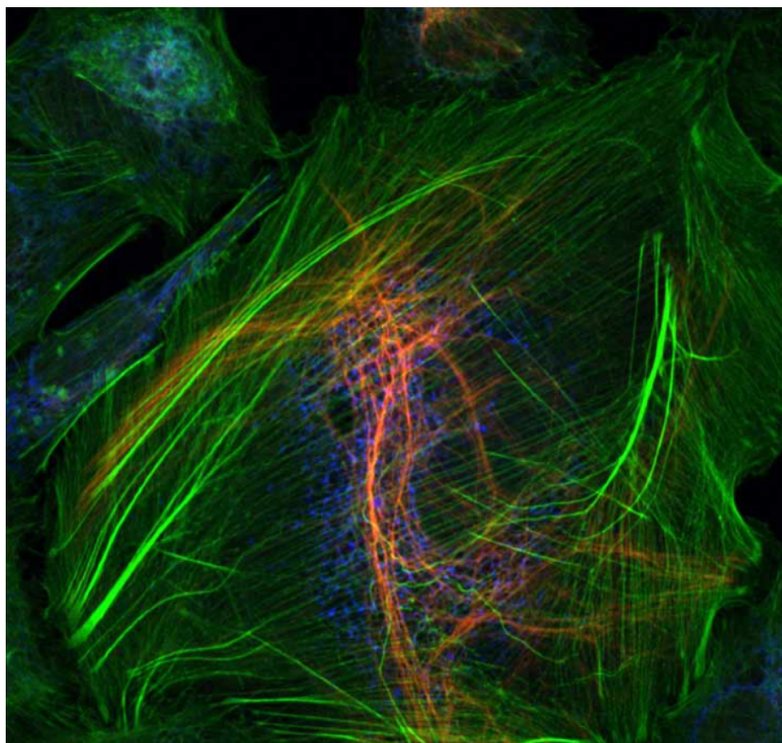

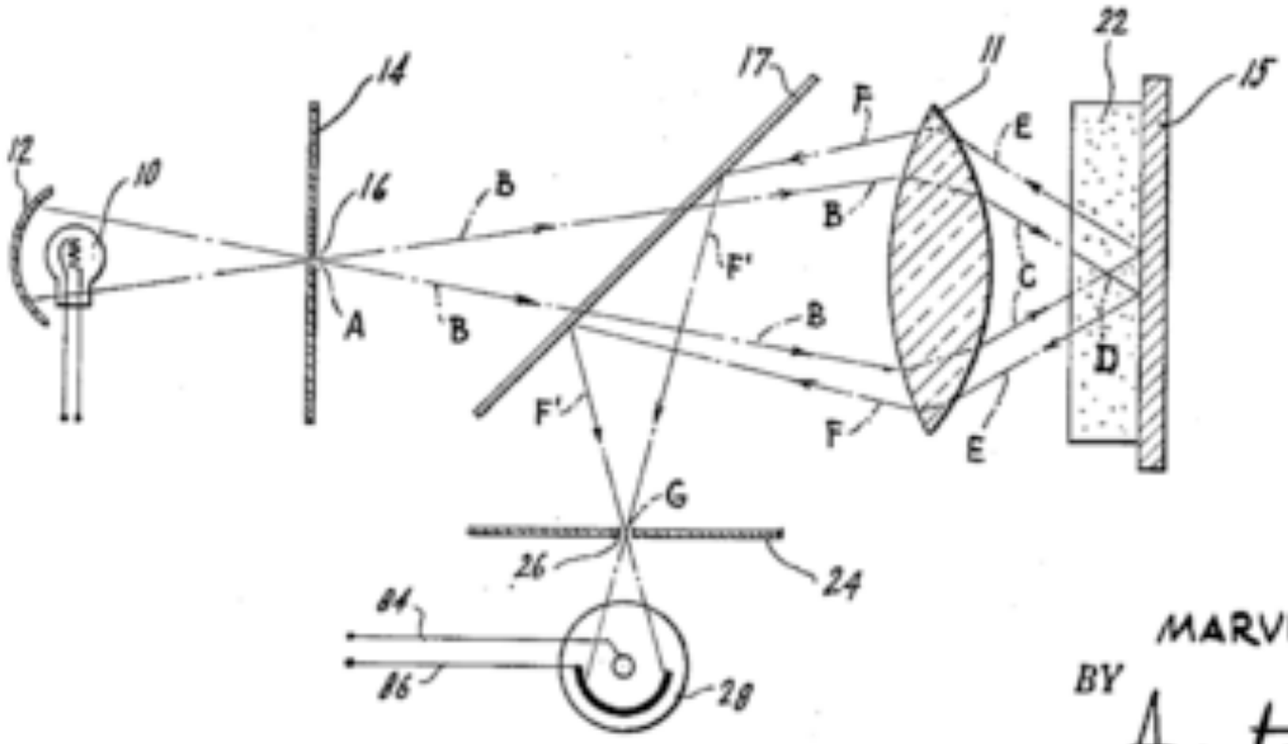

FIG. 3.

INVENTOR.
MARVIN MINSKY

BY Ameter & Levy
ATTORNEYS

Confocal microscope

Wide-field microscopy:

- All of specimen excited at the same time
- Large unfocused background

Confocal microscope:

- Field of view limited by geometric optics
- Pinhole in front of the detector to eliminate out-of-focus signal
- Long exposure required
- Scanning arrangement to build up image of larger region
- Better resolution

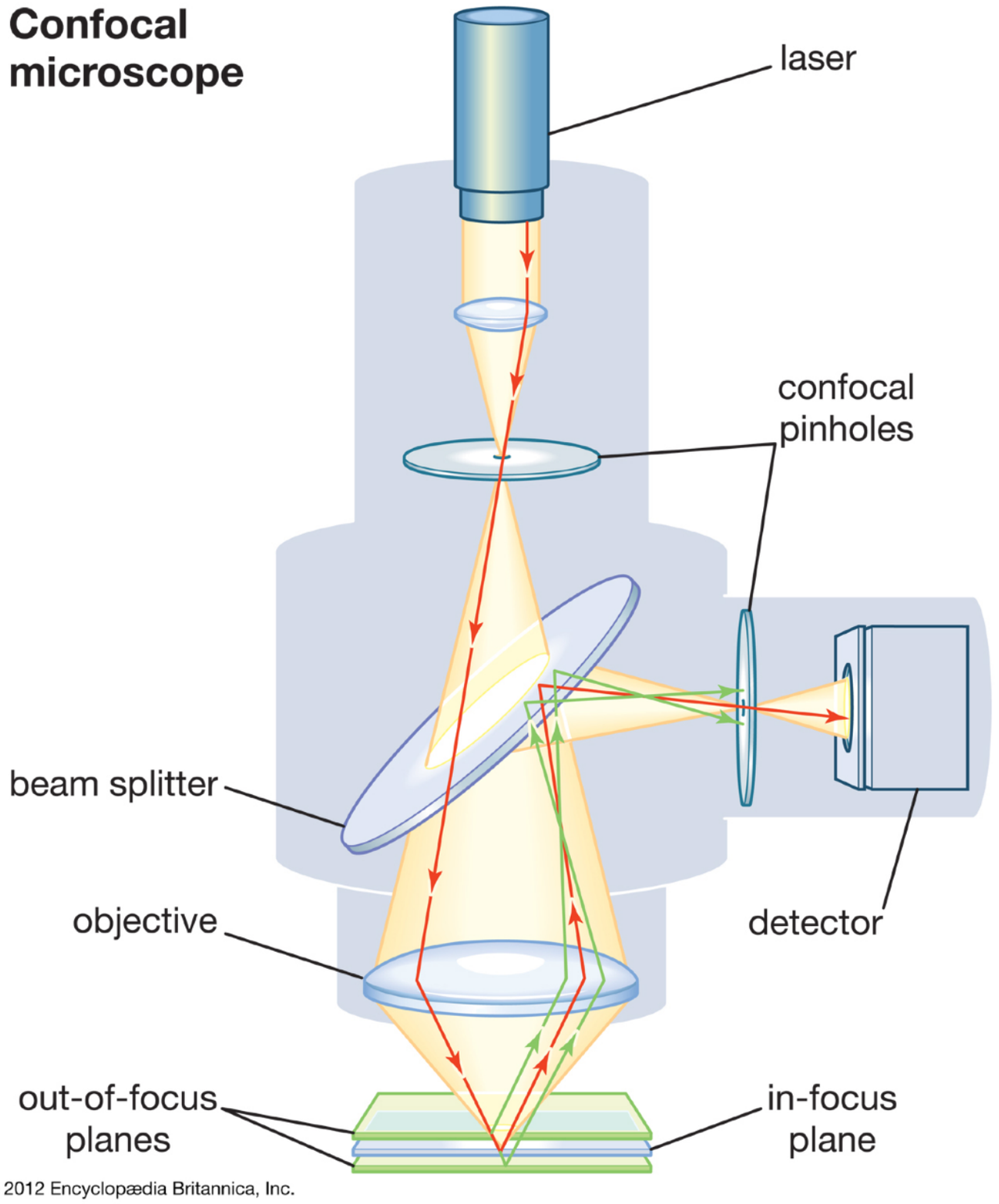

https://www.britannica.com/technology/microscope/Confocal-microscopes

Fluorescent microscope

Fluorescent microscope:

- high intensity light source
- excites a fluorescent species in a sample
- Sample emits different wavelength

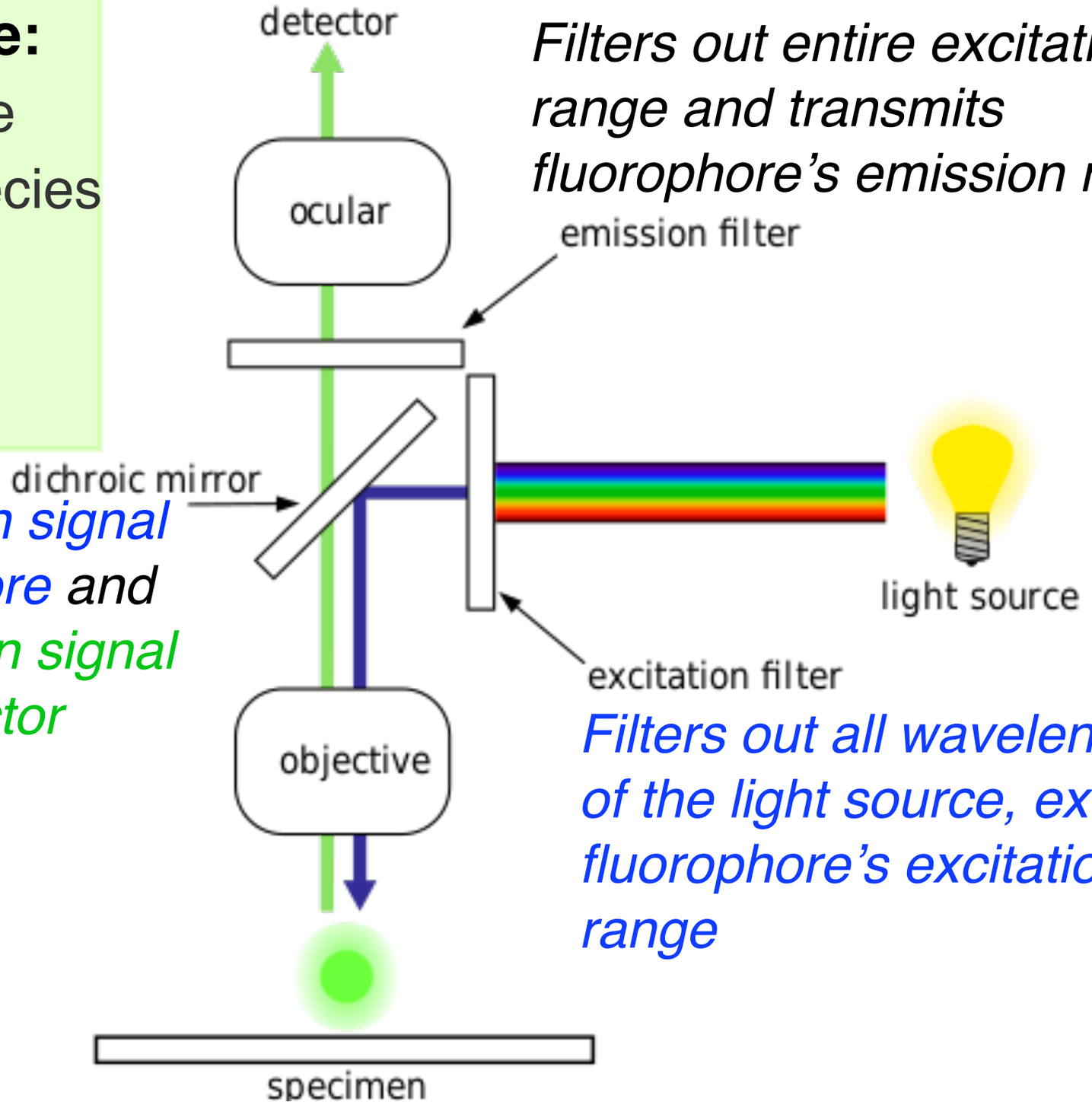

Filters out entire excitation range and transmits fluorophore's emission range

Reflects excitation signal towards fluorophore and *transmits emission signal towards the detector*

Filters out all wavelengths of the light source, except fluorophore's excitation range

Labelled with fluorescent protein (e.g. GFP)

https://www.wikiwand.com/en/Fluorescence_microscope

Confocal fluorescent laser microscope

Fluorescent confocal microscope:

- Combination of two ideas in microscopy technology
- High resolution images
- Life cells
- 2D or 3D through scanning schemes
- Multi-channel through use of range of fluorescent proteins

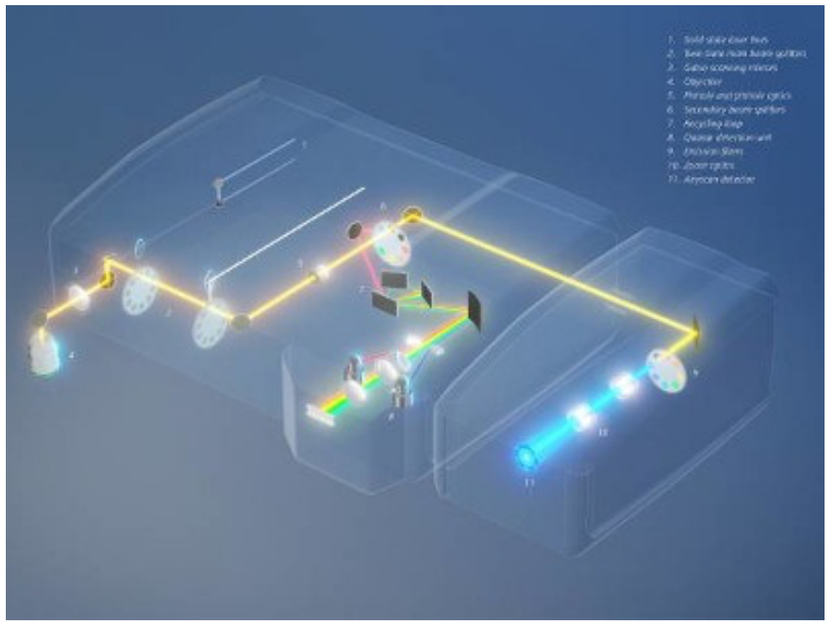

https://www.biocompare.com/25608-Microscopes-and-Cell-Imaging-Systems/14617250-ZEISS-LSM-980-Confocal-Laser-Scanning-Microscope/?pda=25608|14617250_0_1|2254289,2254327|1|&dfp=true

https://en.wikipedia.org/wiki/Green_fluorescent_protein#/media/File:Fluorescence_from_Fluorescent_Proteins.jpg

Example: Quantifying protein abundance in their actual locations in cells

Sub-cellular localisation of tumour antigen SSX2IP in leukemia cells

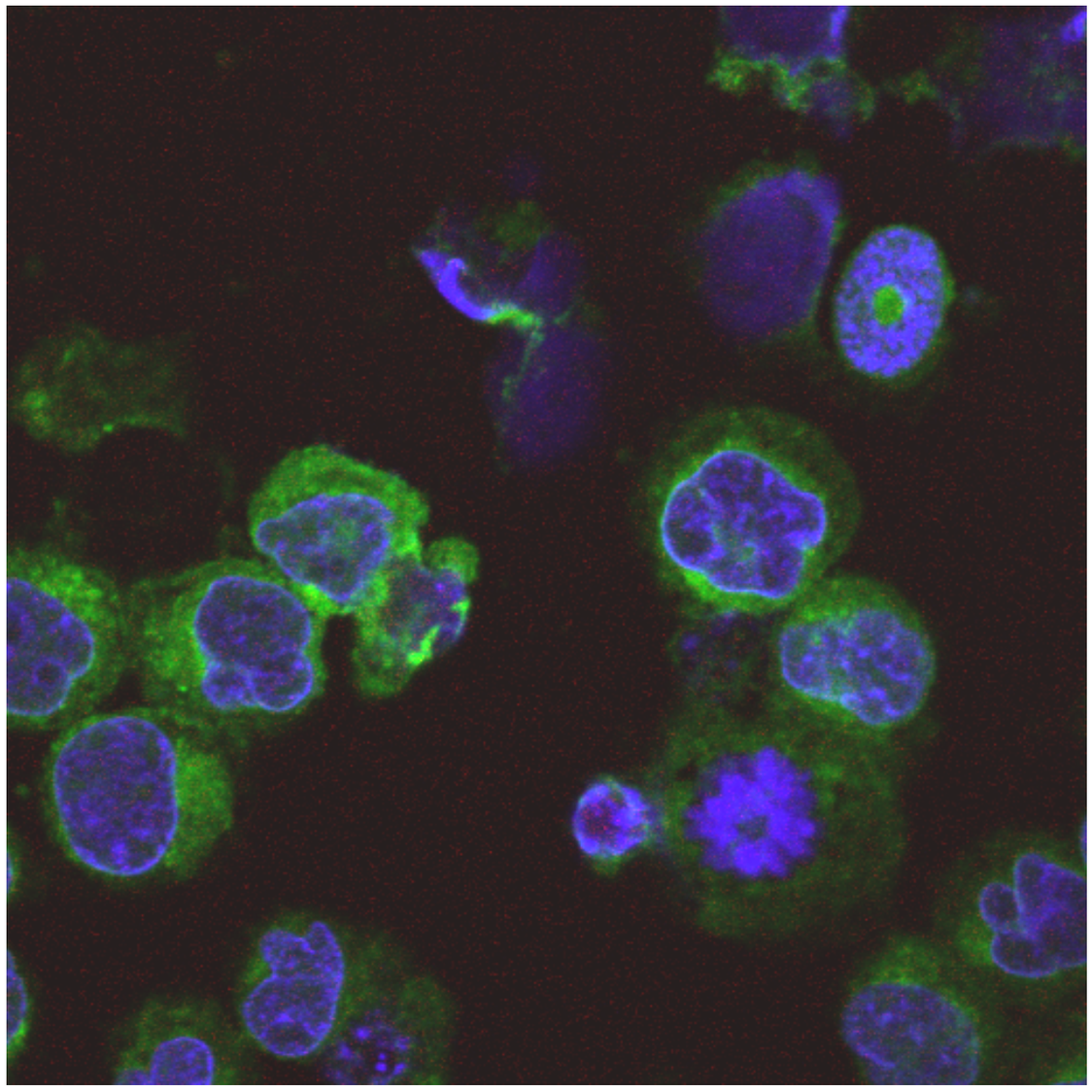

Green: SSX2IP expression visualised by anti-SSX2IP-fluorescein isothiocyanate on the cell's surface.

Blue: Stained Cell nuclei using 4,6'-diamino-2-phenylindole (DAPI).

Protocol of the experiment:
Leukaemia cell line K562 air dried for 4-18hours onto glass microscope slides, stored at -20°C wrapped in saranwrap, defrosted, stained with antigen specific primary, and fluorescently labelled secondary antibodies.

http://www.intechopen.com/books/novel-gene-therapy-approaches/identification-and-validation-of-targets-for-cancer-immunotherapy-from-the-bench-to-bedside

Example:
3 components in dividing human cancer cells

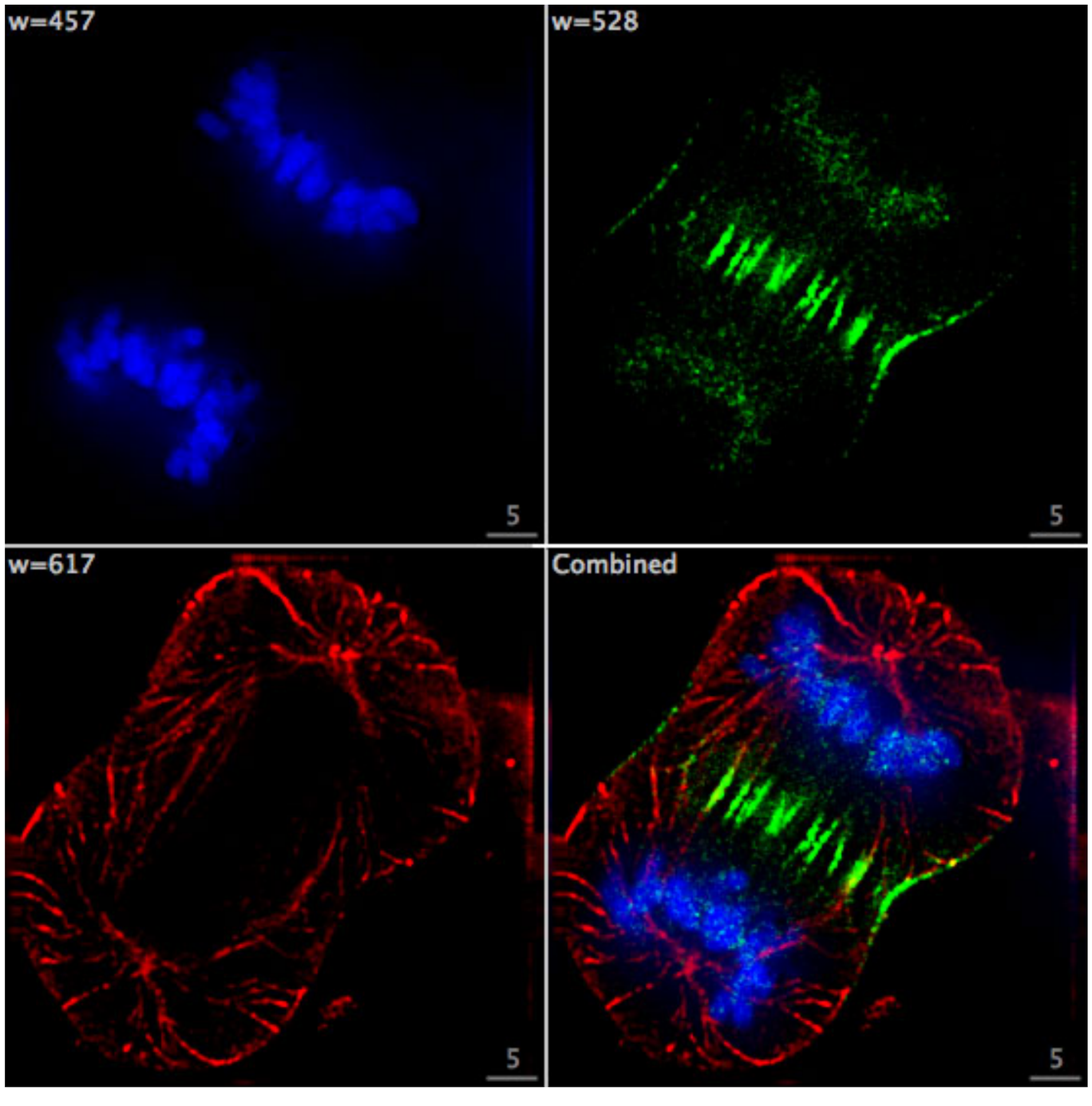

Scanning scheme for fluorescent imaging:

- Blue: Chromosomes (DNA)
- Green: INCENP (protein)
- Red: microtubules
- Fluorophores imaged separately using different excitation and emission filters
- Images captured sequentially
- Overlaid

Microtubules formation during mitosis

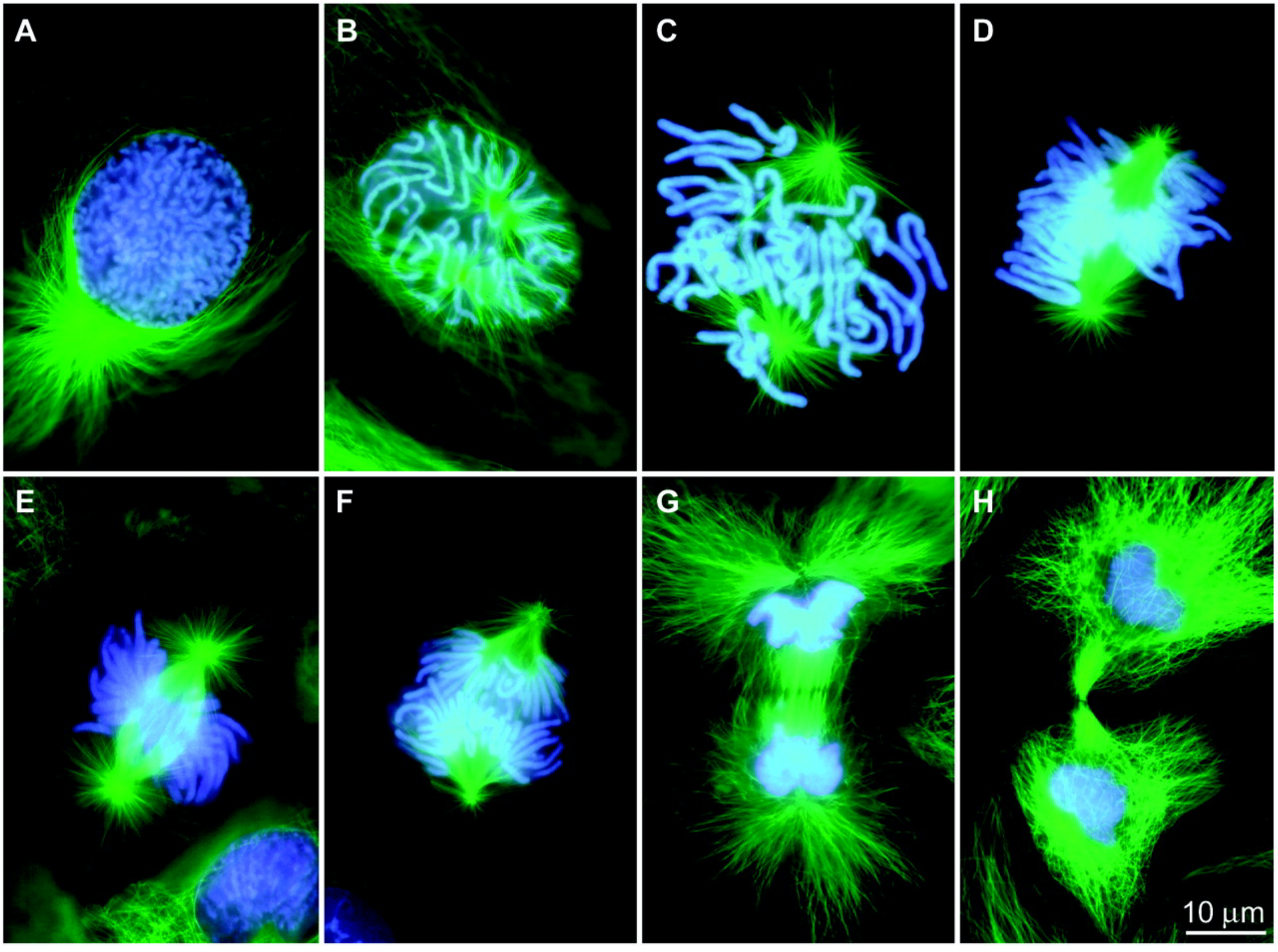

https://science.sciencemag.org/content/300/5616/91/tab-figures-data

Microtubules during mitosis (cell division)

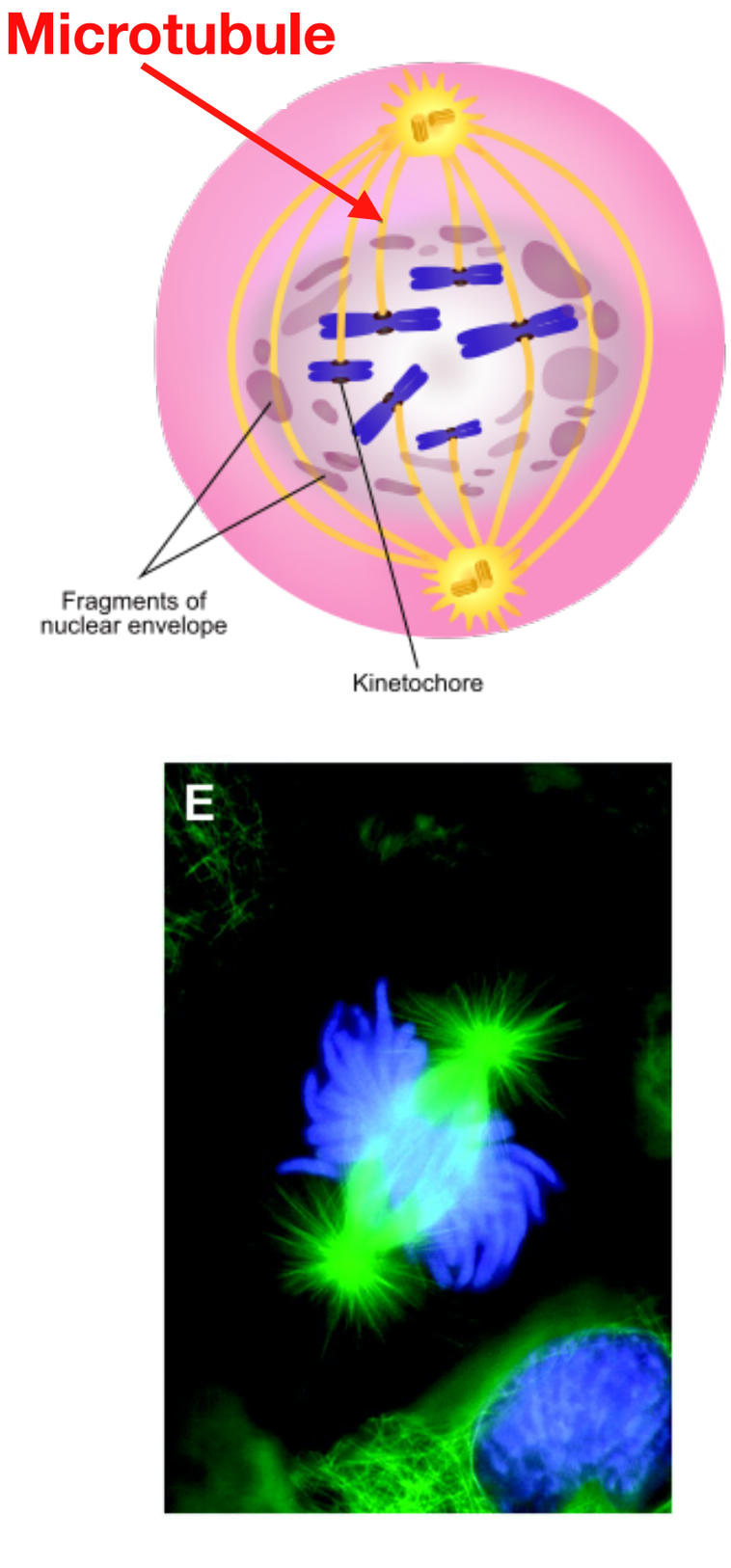

- Centrosomes = centrioles + microtubules
- Centrioles help the spindle into proper formation
- Spindle microtubules are arranged in K-fibers
- Intertubule bridges formed by mesh

Perpendicular to the microtubule axis

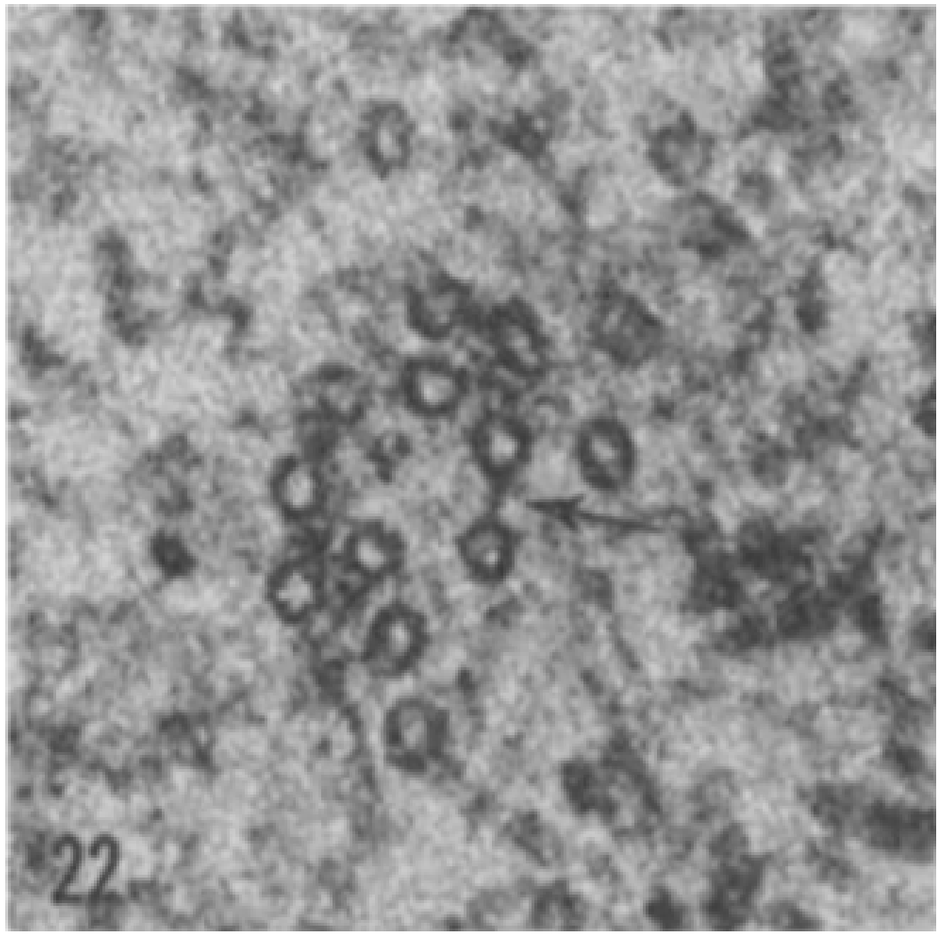

Parallel

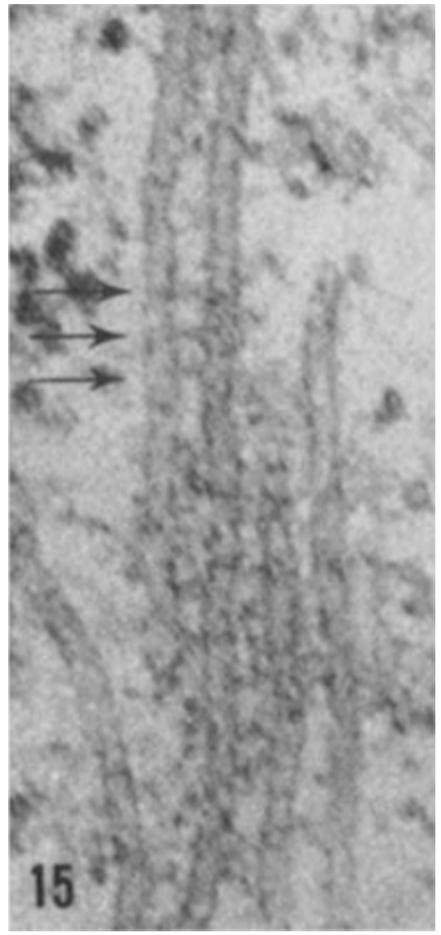

https://www.scienceabc.com/nature/mitosis-vs-meiosis-how-does-cell-division-work.html

Microtubules locations as point patterns

Stephen Royle's Lab (Centre for Mechanochemical Cell Biology) asks:
What is the role of TACC3 protein for the structure of microtubules within K-fibres and mesh?

Experiment: Overexpression of TACC3 through treatment versus control.

Data: Microscopic images collected in planes perpendicular to the fibre axes.

Perpendicular view

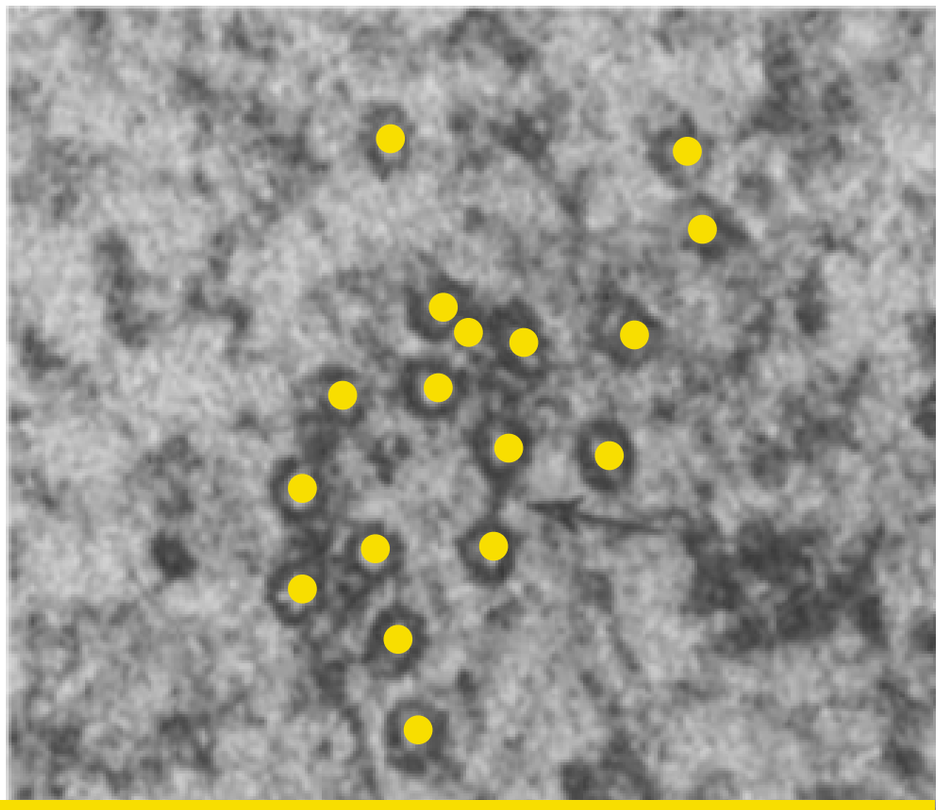

Model: locations as point pattern

Parallel

Mesh

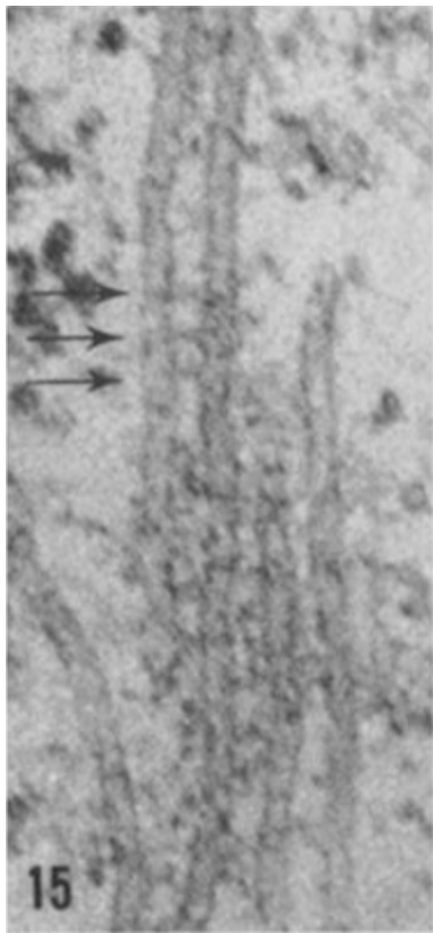

Describing and comparing protein abundance

Data:

Point patterns $\underline{x}^I$, $I = I_0 \cup I_1$.

Model:

Point patterns $\underline{x}^{I_0}$ independent realisations of point process $\underline{X}^0$.

Point patterns $\underline{x}^{I_1}$ independent realisations of point process $\underline{X}^1$.

Task:

Inference on existence and form of a difference between $\underline{X}^0$ and $\underline{X}^1$.

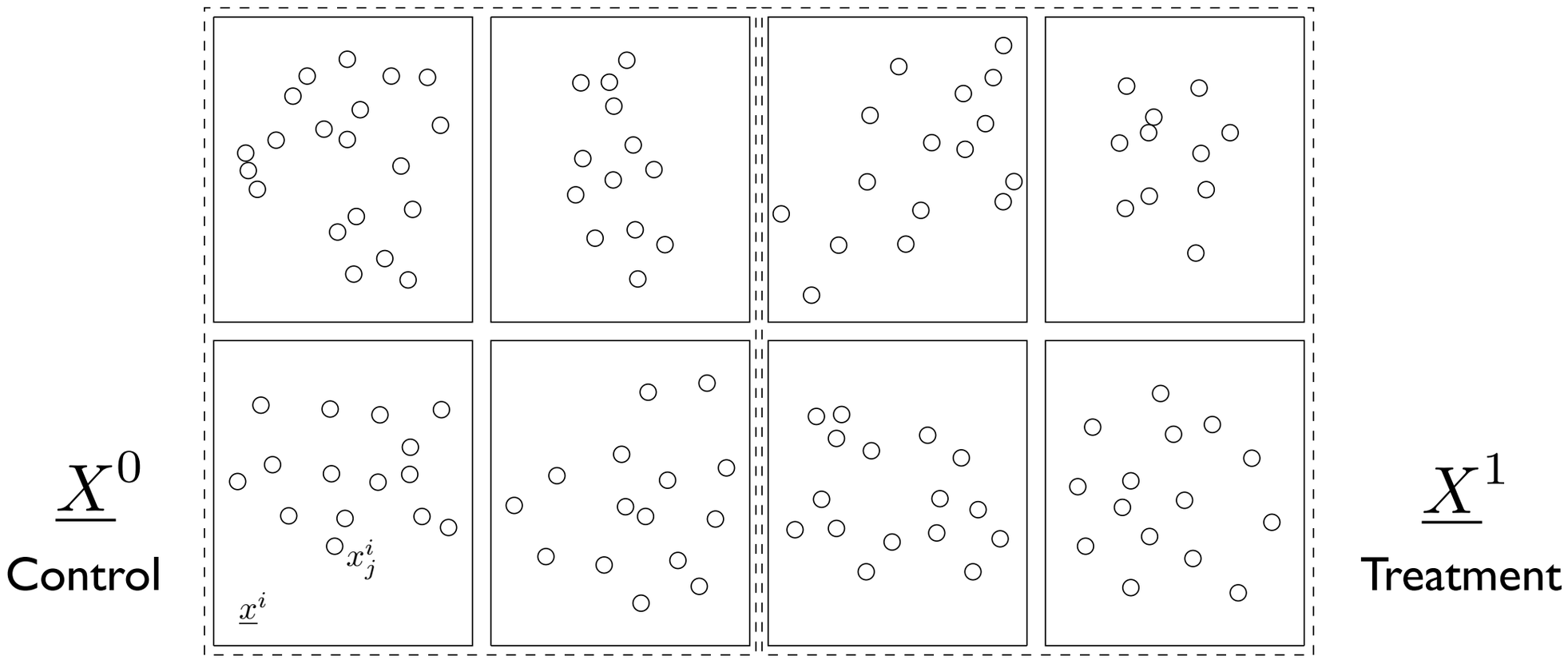

Point patterns models

Set of point patterns:

$$\chi_2 := \{(\underline{x} = x_1, x_2, \ldots, x_{n(\underline{x})}) : n(\underline{x}) \in \mathbb{N}, x_i \in \mathbb{R}^2 \text{ for } i = 1, 2, \ldots, n\}$$

Model pattern as realisations of a point process:

Random subset $\underline{X}$ on $\mathbb{R}^2$.

For B in Borel σ-algebra $\mathcal{B}(\mathbb{R}^2)$ on $\mathbb{R}^2$: $\underline{X}_B = \underline{X} \cap B$

Counts (random variable): $N(B) = n(\underline{X}_B) =$ number of points of $\underline{X}$ in B

Intensity measure μ

$$\mu(B) = \mathbb{E}[N(B)], \quad \forall B \in \mathcal{B}(\mathbb{R}^d).$$

If for some function $\rho : \mathbb{R}^2 \to [0, \infty)$

$$\mu(B) = \int_{x \in B} \rho(x) dx, \quad \forall B \in \mathcal{B}(\mathbb{R}^d),$$

then ρ is referred to as the intensity function of $\underline{X}$.

Summary statistics: basics

Let $\underline{x}$ be a realisation of $\underline{X}$ on the observation window W.

Estimator for the **intensity** of $\underline{X}$:

$$\hat{\rho} = \frac{n(\underline{x})}{|W|}$$

Let $\mathrm{nn}(x_j)$ be the (set of) nearest neighbours of point x_j.

$$\mathrm{nn}(x_j) = \{x_k : k = \mathrm{argmin}_l ||x_l - x_j||\},$$

and $\mathrm{nnd}(x_j)$ its nearest neighbour distance

$$\mathrm{nnd}(x_j) = \inf_{x \in \mathrm{nn}(x_j)} \{||x_j - x||\}.$$

Estimator for the **mean nearest neighbour distance** for $\underline{X}$:

$$\overline{\mathrm{nnd}}(\underline{x}) = \frac{1}{n(\underline{x})} \sum_{j=1}^{n(\underline{x})} \mathrm{nnd}(x_j)$$

Summary statistics: K-function

K-function (Ripley 1977) (scaled neighbourhood count function):

$$K(r) = \frac{1}{\rho}\mathbb{E}\left[\frac{1}{N(S)}\sum_{x_j \neq x_k \in \underline{X}} 1_{\{||x_j - x_k|| < r\}}\right]$$

Estimate:

$$\hat{K}(\underline{x}, r) = \frac{|W|}{n(\underline{x})^2}\sum_{j \neq k} e_{j,k} 1_{\{||x_j - x_k|| \leq r\}}$$

where $e_{j,k}$ is the proportion of the circumference of the circle with centre x_j and radius $||x_j - x_k||$ in W (edge correction).

$K(r) = \pi r^2$: CSR (complete spatial randomness)

$K(r) > \pi r^2$: aggregation at distances less than r

$K(r) < \pi r^2$: repulsion at distances less than r

Summary statistics: G-function

Nearest neighbour function (Diggle 2003):

$$G(r) = \frac{1}{\rho|B|}\mathbb{E}\left[\sum_{x\in \underline{X}_B} 1_{\{\underline{X}\setminus x)\cap b(x,r)\neq 0\}}\right]$$

for finite B in $\mathbb{R}^2$, and $b(x,r)$ the disc centred at x with radius r.

(For stationary $\underline{X}$ it is independent of B.)

Distribution of distance of randomly selected point to its nearest neighbour.

Estimate:

$$\hat{G}(\underline{x},r) = \frac{1}{n(\underline{x})}\sum_{j=1}^{n(\underline{x})} 1_{\{\mathrm{nnd}(x_j)\leq r\}}$$

If $\underline{X}$ is completely spatially at random then $G(r) = 1-\exp(-\rho\pi r^2)$

Excursion:
Point process models of dead pixels

Modern computed tomography uses digital detectors

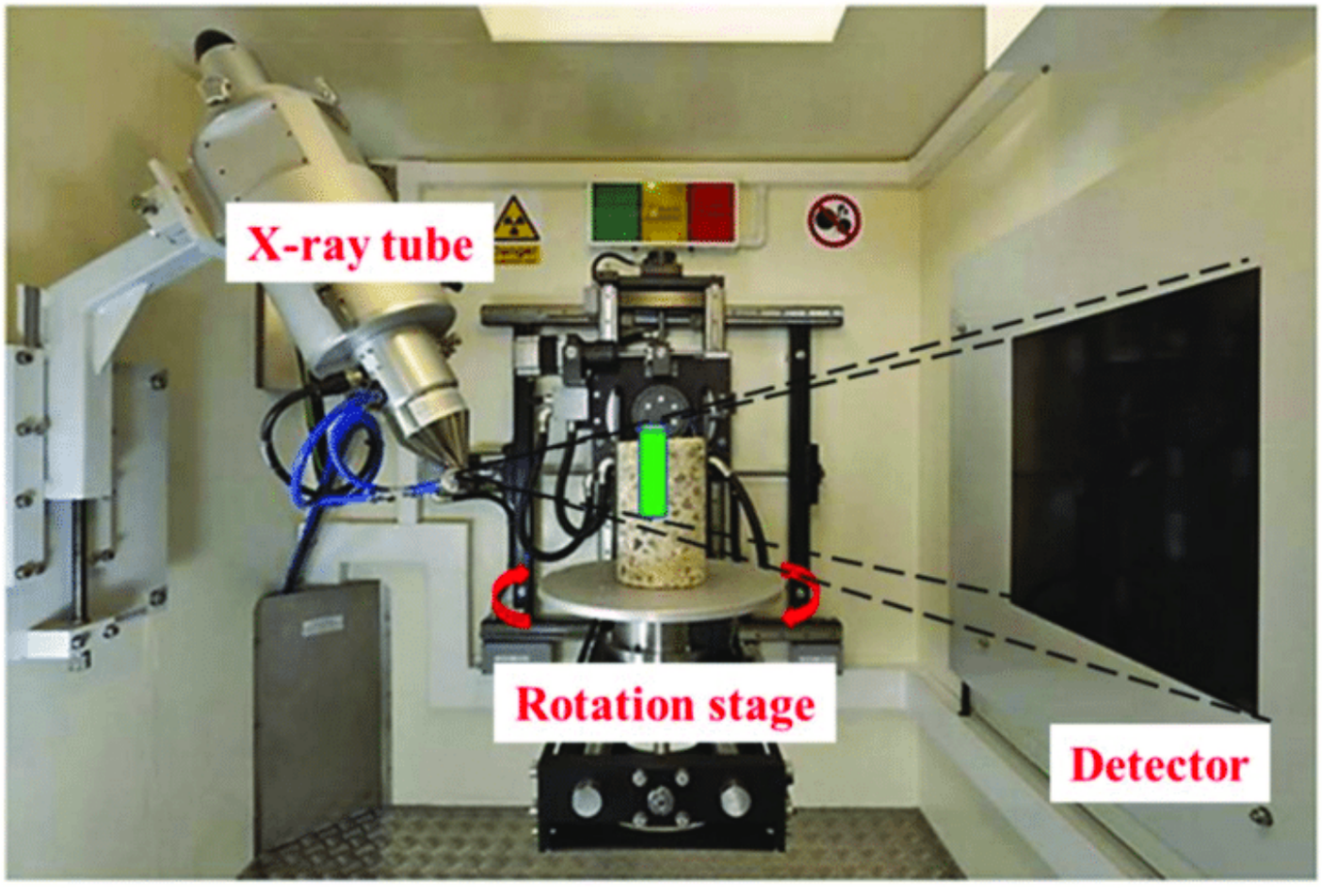

https://www.researchgate.net/figure/Example-of-an-industrial-computed-tomography-CT-system_fig1_324511614

X-ray detector

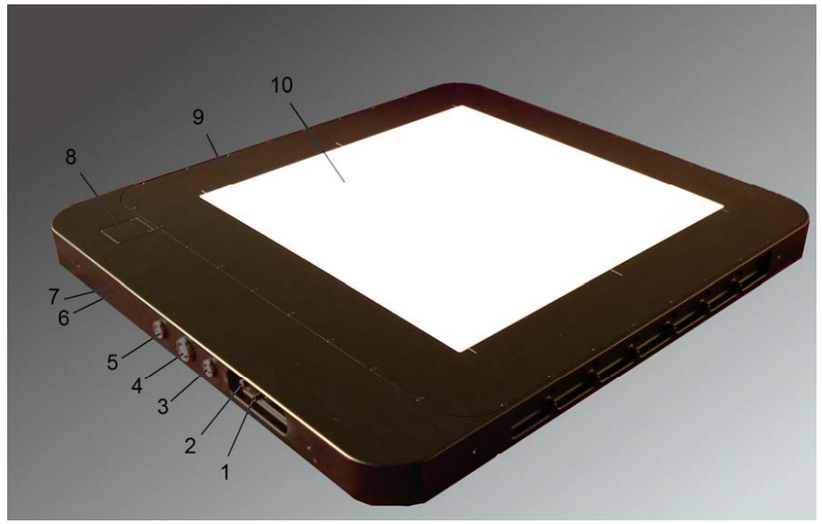

Perkin Elmer
XRD 1621

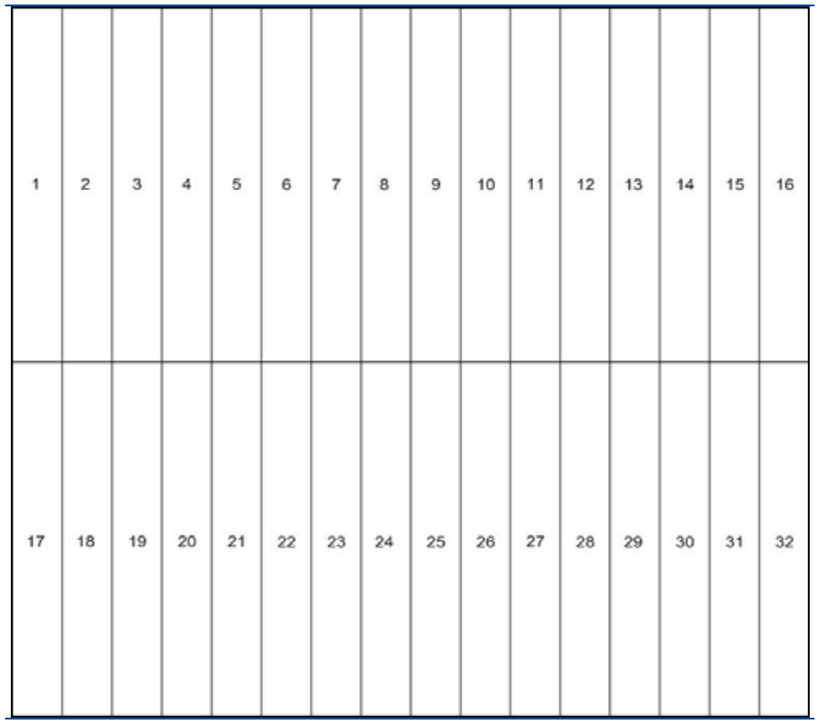

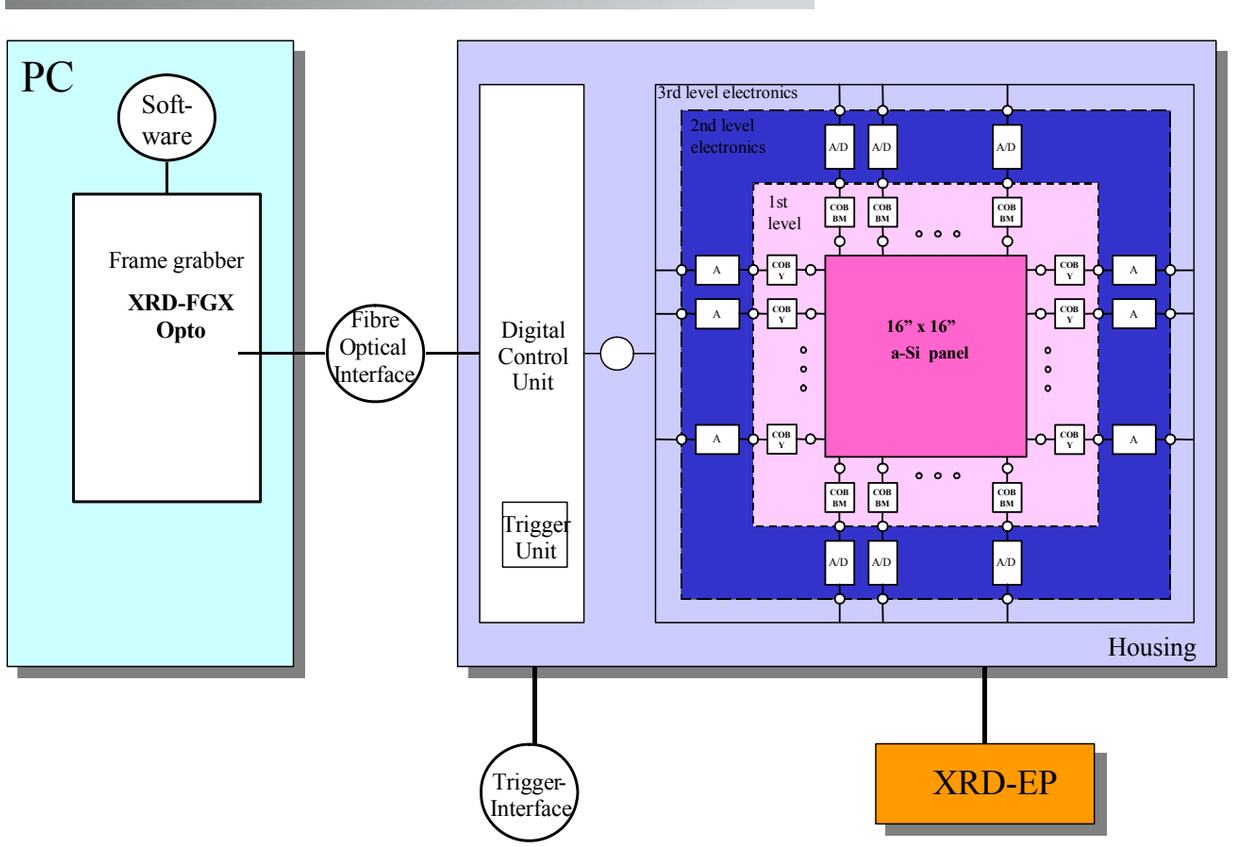

Readout groups (ROG):
Upper groups transferred first, starting read out from the upper row.
Lower groups starting from the last row.

Bad pixel maps

- Criteria for "underperforming" (Perkin Elmer):
  - Signal sensitivity (at different energies)
  - Noise observed in sequence of 100 bright/dark images
  - Uniformity (global, local)

- Each bad pixel map consist of a total of 10 files:
  - White images: mean, min, max, sd (.tif)
  - Grey images: mean (.tif)
  - Black images: mean, min, max, sd (.tif)
  - Bad pixel list of locations (.xml)

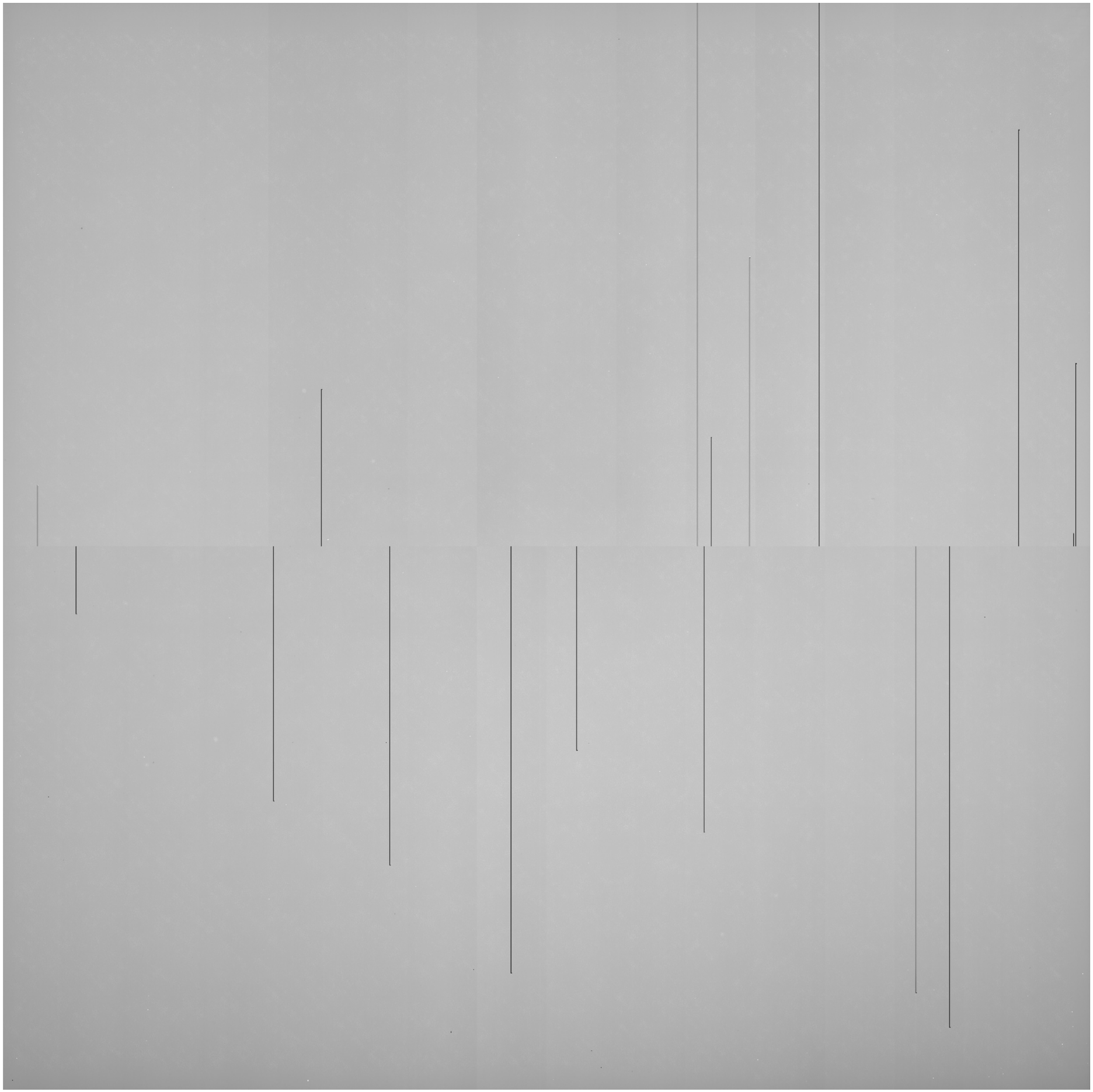

Horizontal midline

A_0: White image from bpm folder

Local defects: Dead lines

- Lines on bad pixel images
- From centre horizontal line outwards
- Visible on tif images of channel(s), too

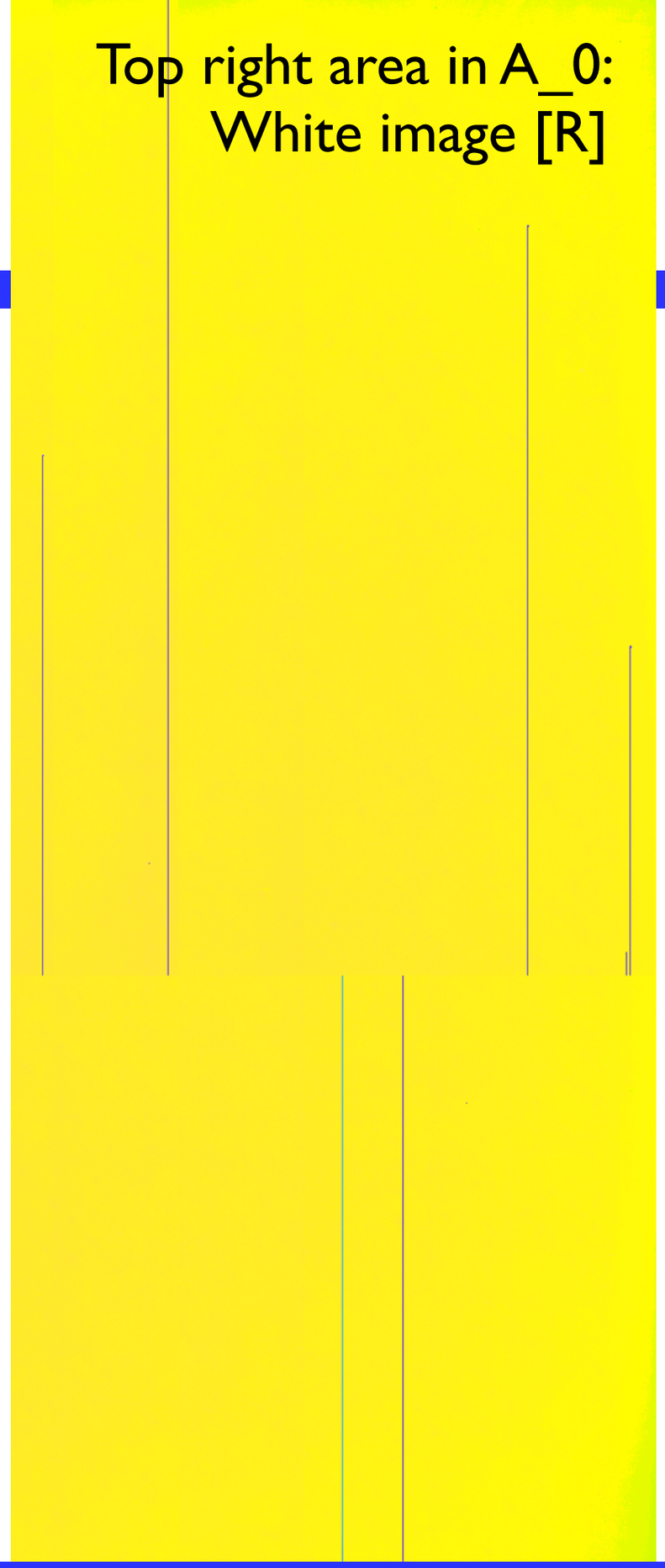

Local defects: Isolated dead pixels

Singles, doubles, small clusters

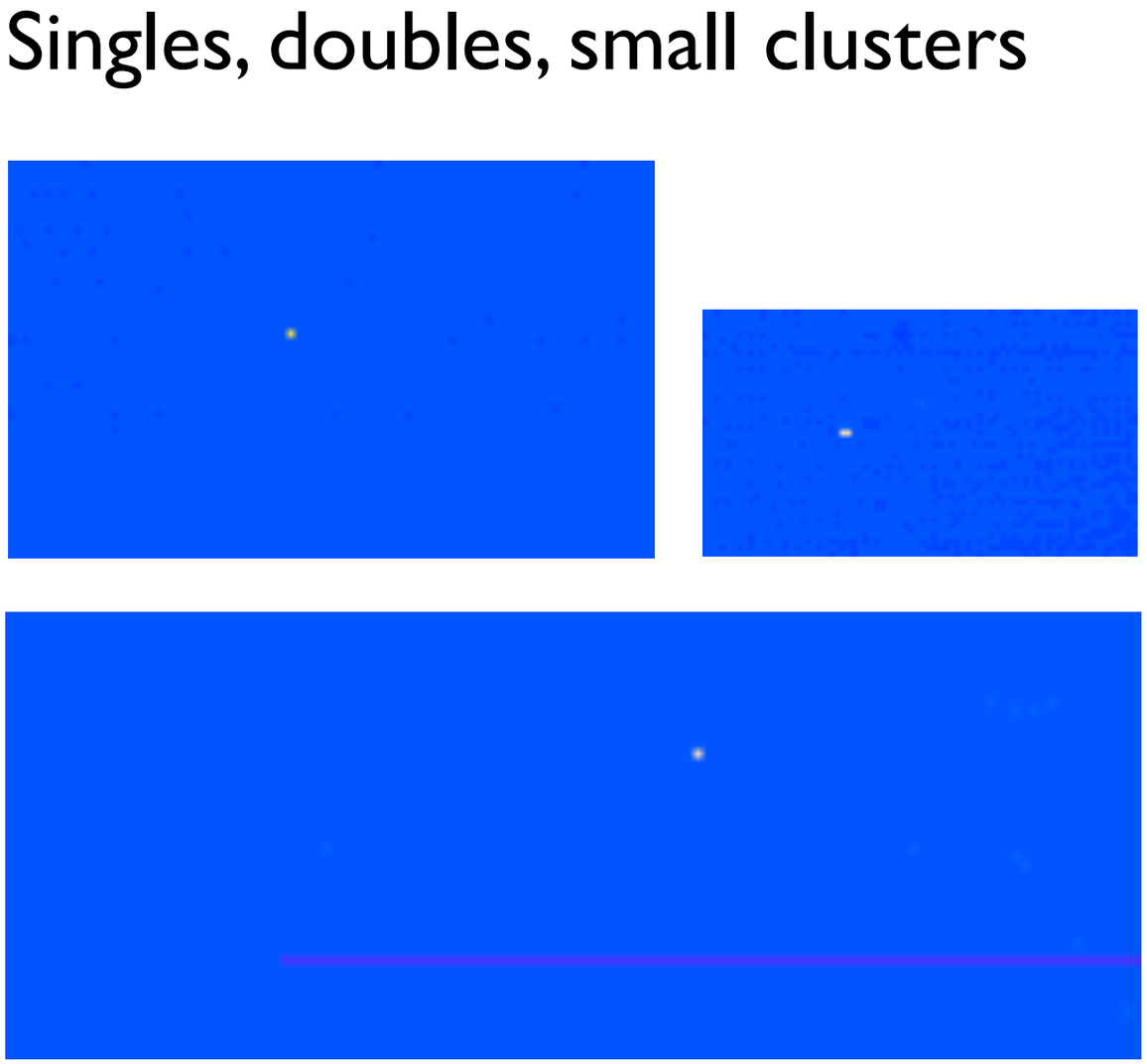

A_0: Grey image [R]

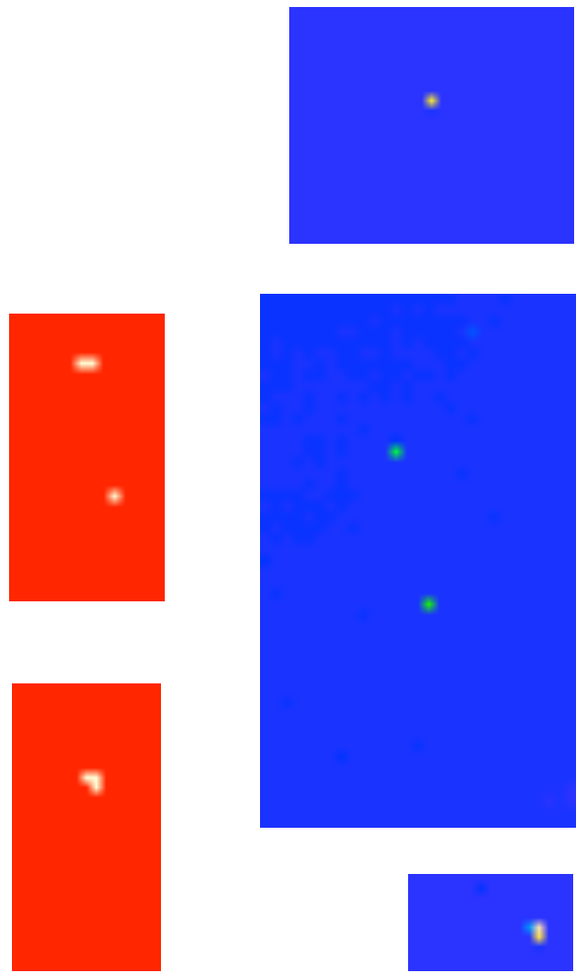

A_0:
bp binary
image [R]

A_0: Black
image [R]

Local defects: Corners

B_0: Binary bad pixel image [R]

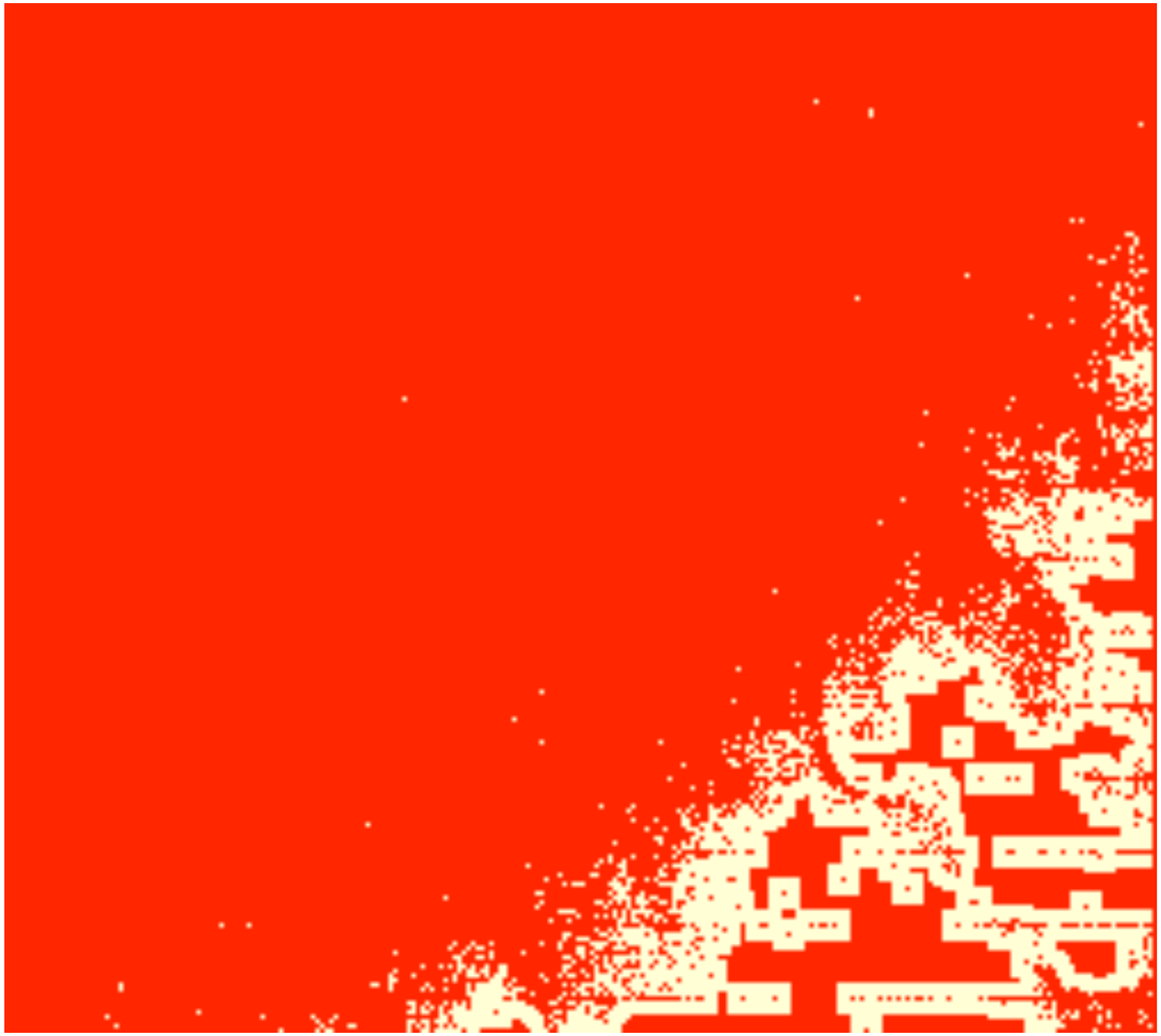

Local defects: Ends of dead lines

bmp binary image

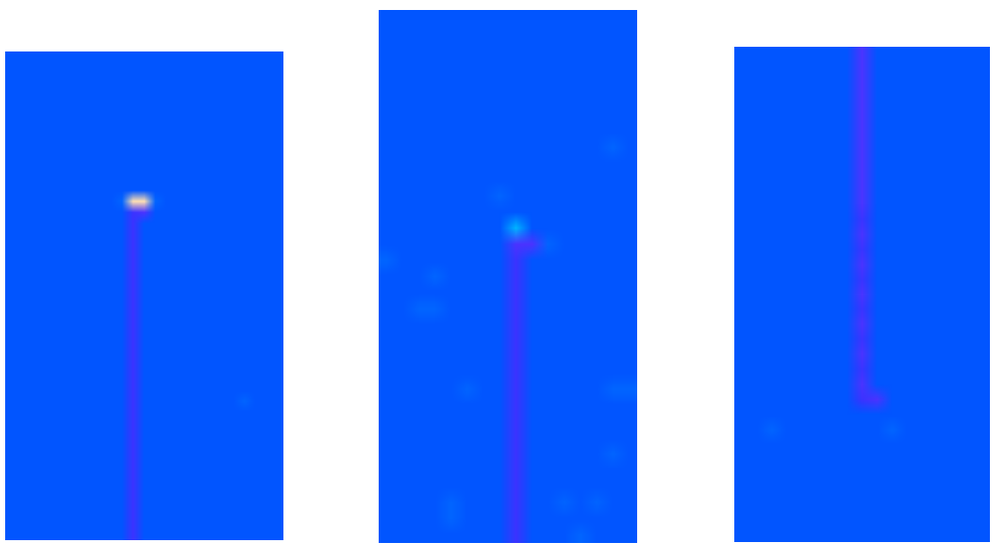

Black image

- Most lines end in small cluster pointing to the right
- Lines are composed of dark pixels
- Lines have constant intensity, except end may differ

Local defects: Patches

- Areas with high density area of bad pixels

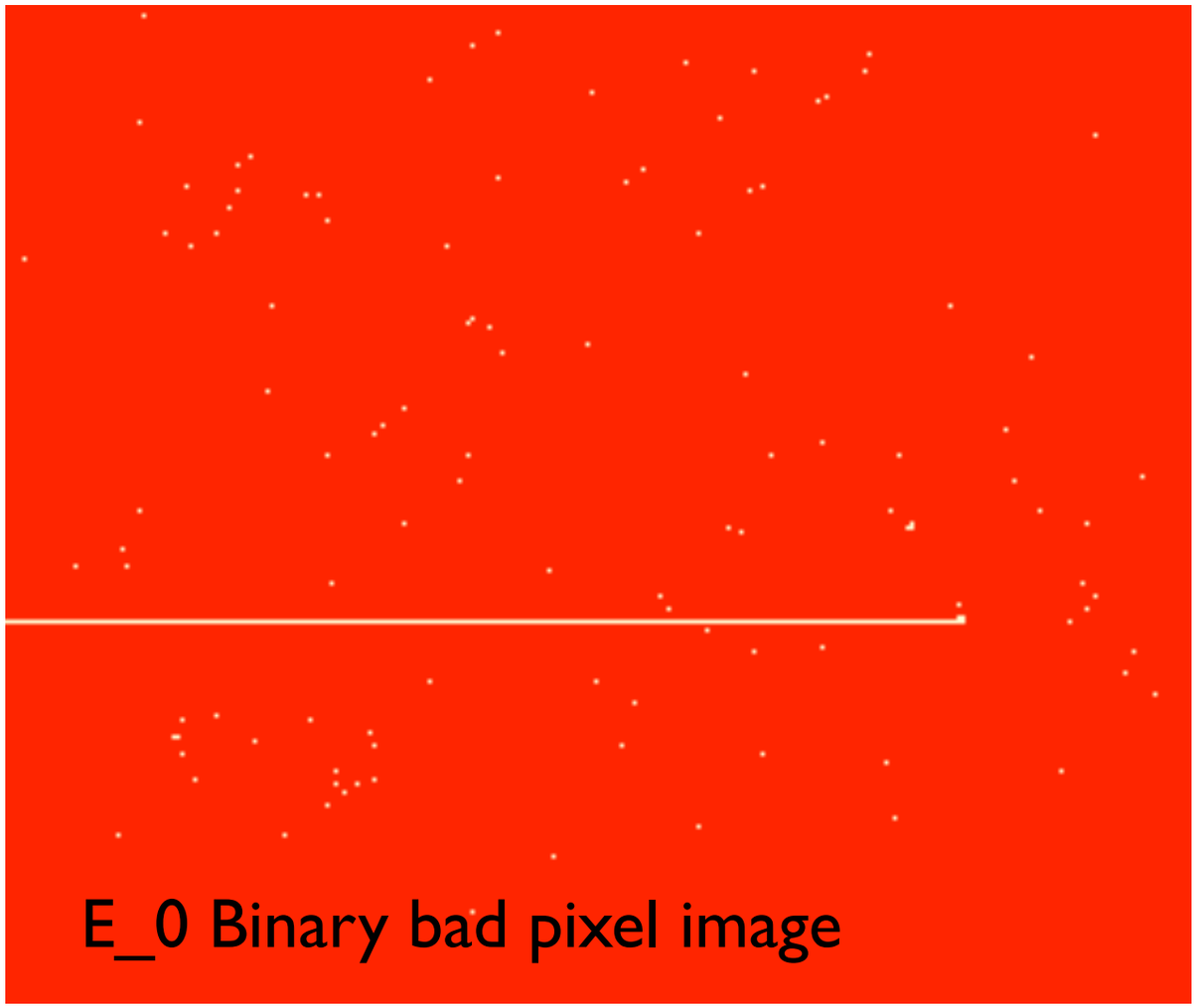

E_0 Binary bad pixel image

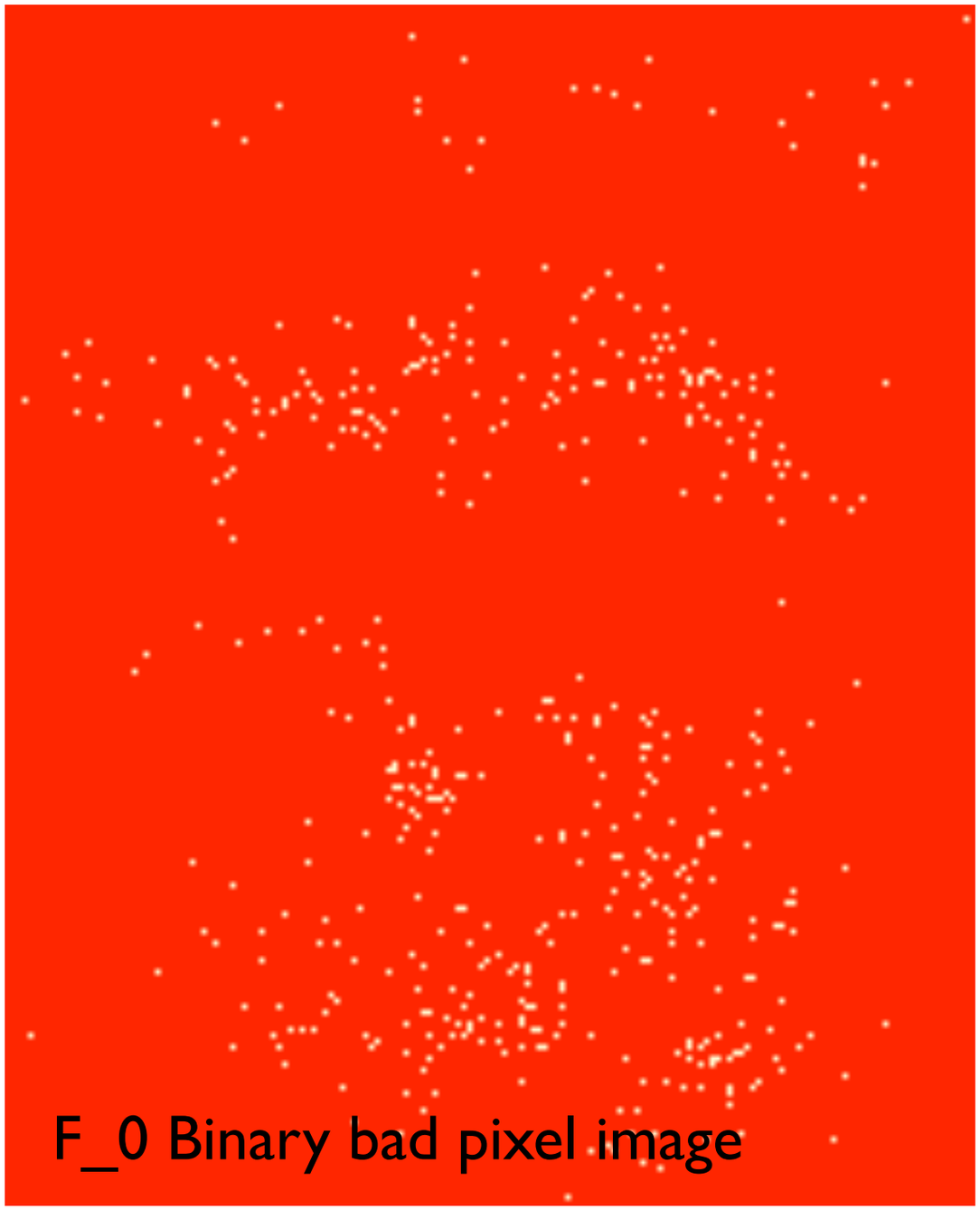

F_0 Binary bad pixel image

Point pattern and K-function

K-function: for h>0, K(h) is the **expected number of extra points in circle of radius h, rescaled by density**

$$K(h) = \frac{1}{\lambda} E[N(C_h - \{s\}) \mid N(s) = 1]$$

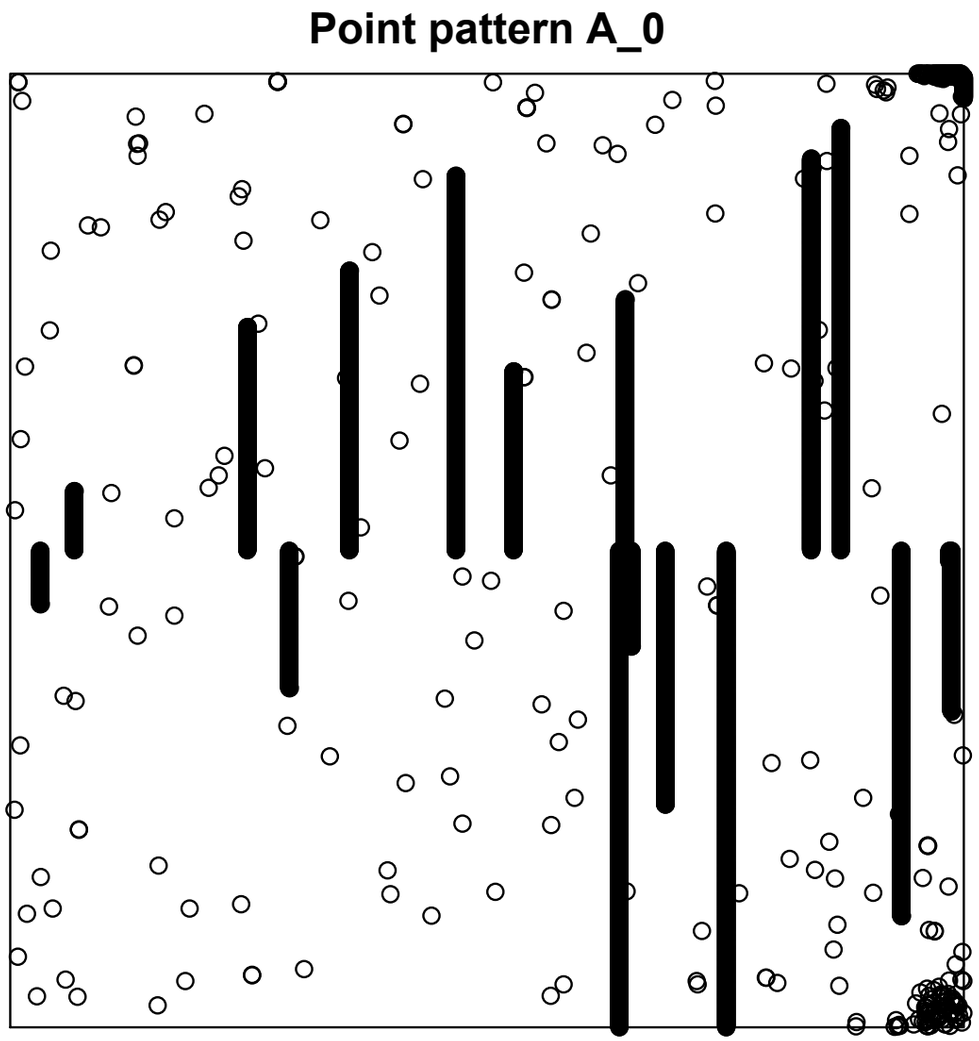

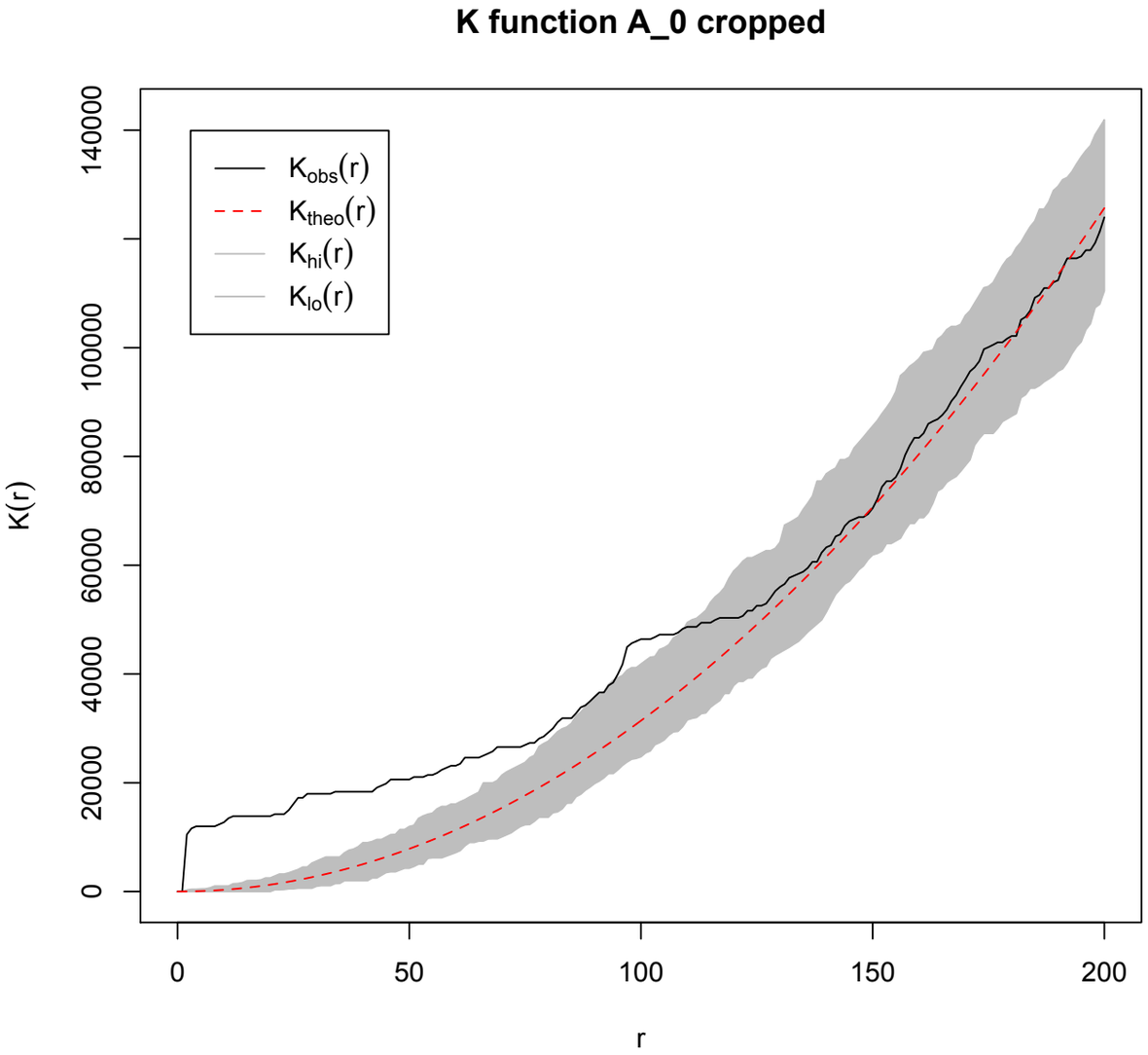

Point pattern and K-function

K-function: for h>0, K(h) is the **expected number of extra points in circle of radius h, rescaled by density**

$$K(h) = \frac{1}{\lambda} E[N(C_h - \{s\}) \mid N(s) = 1]$$

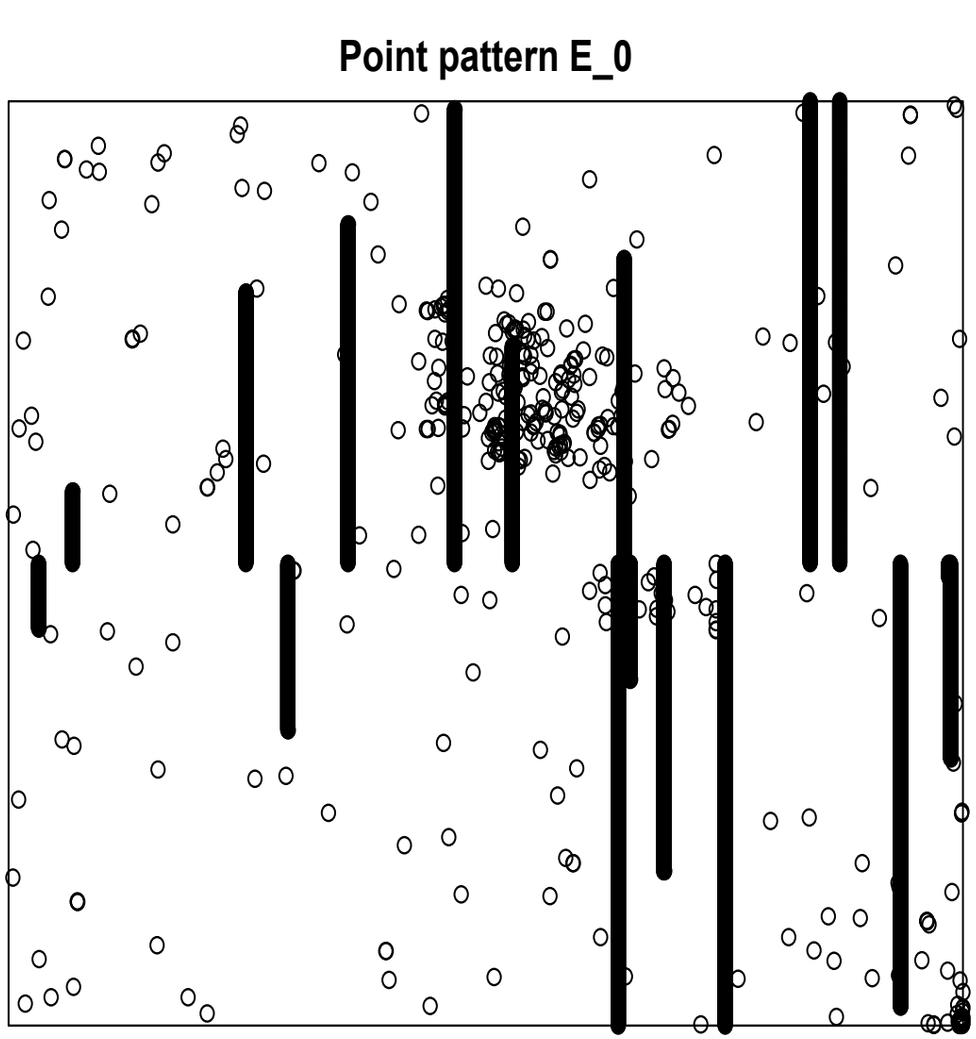

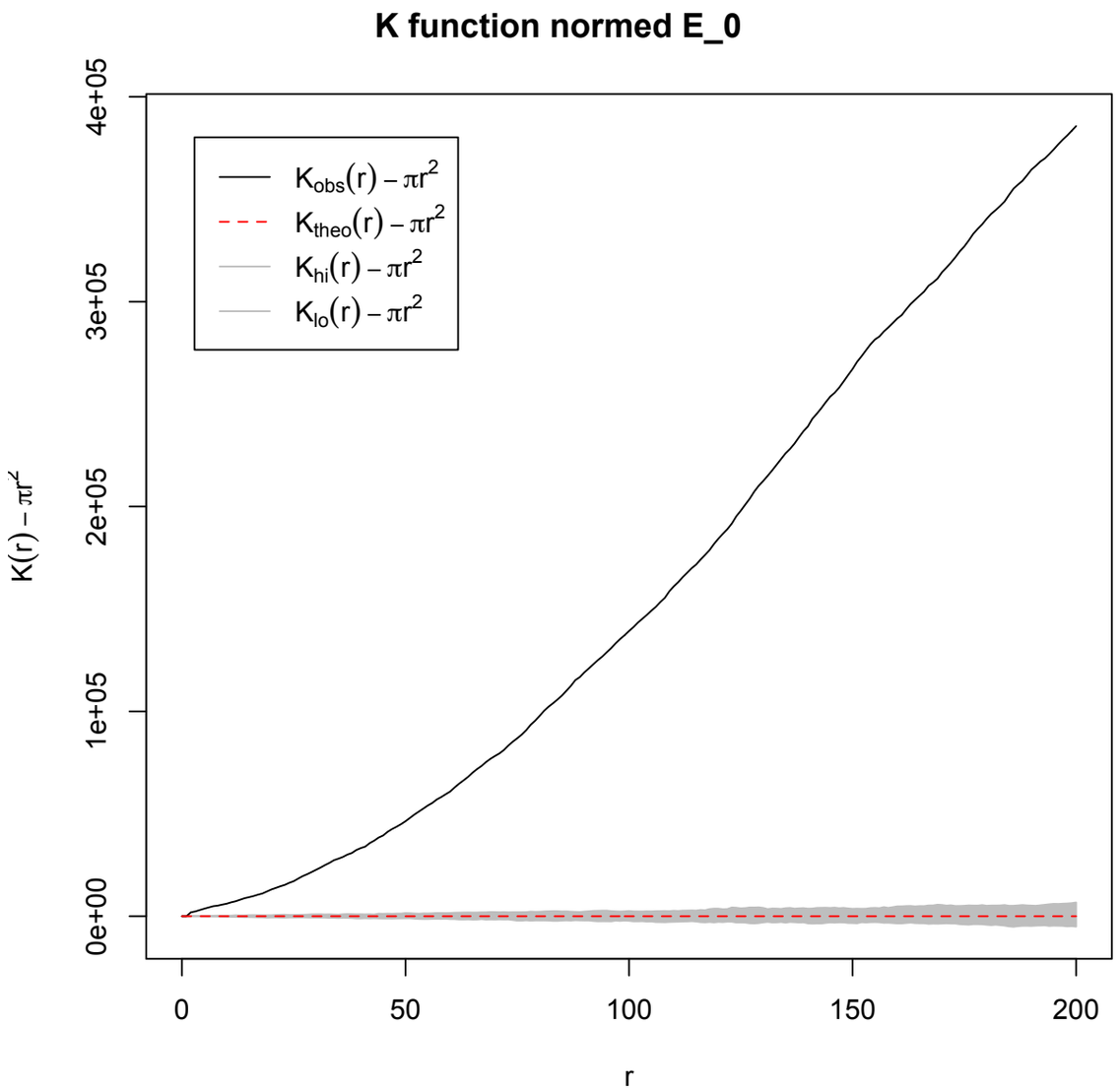

Question

Is it CSR after we remove all specific problems?

Step 1:
Convert point process into *event process* by

- Reducing lines to their endpoint
- Reducing clusters to their centre point

Step 2:

- Fit inhomogeneous density
- Cut out areas above threshold

Higher level defect model (Step 1)

Conversion of point process to *event process*

Defect pixels

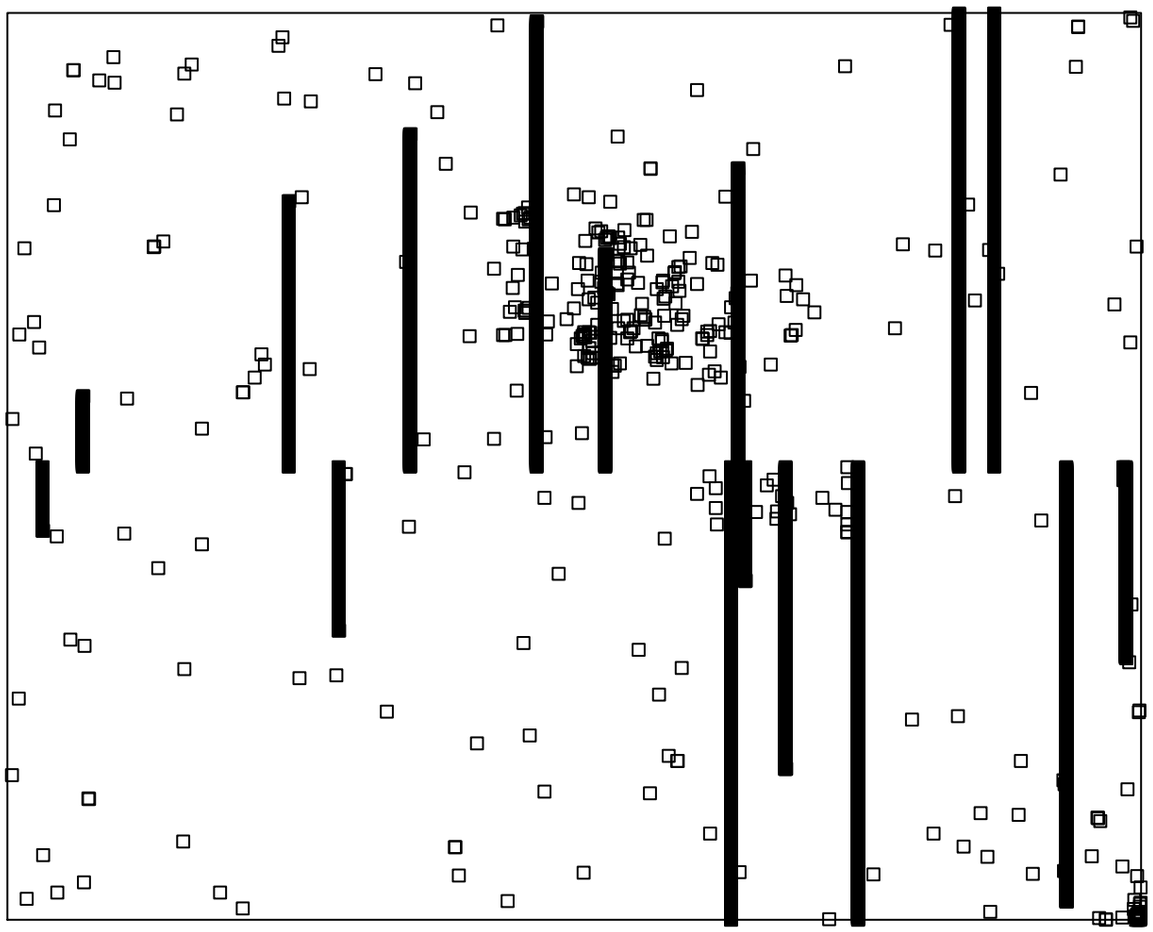

Defect events

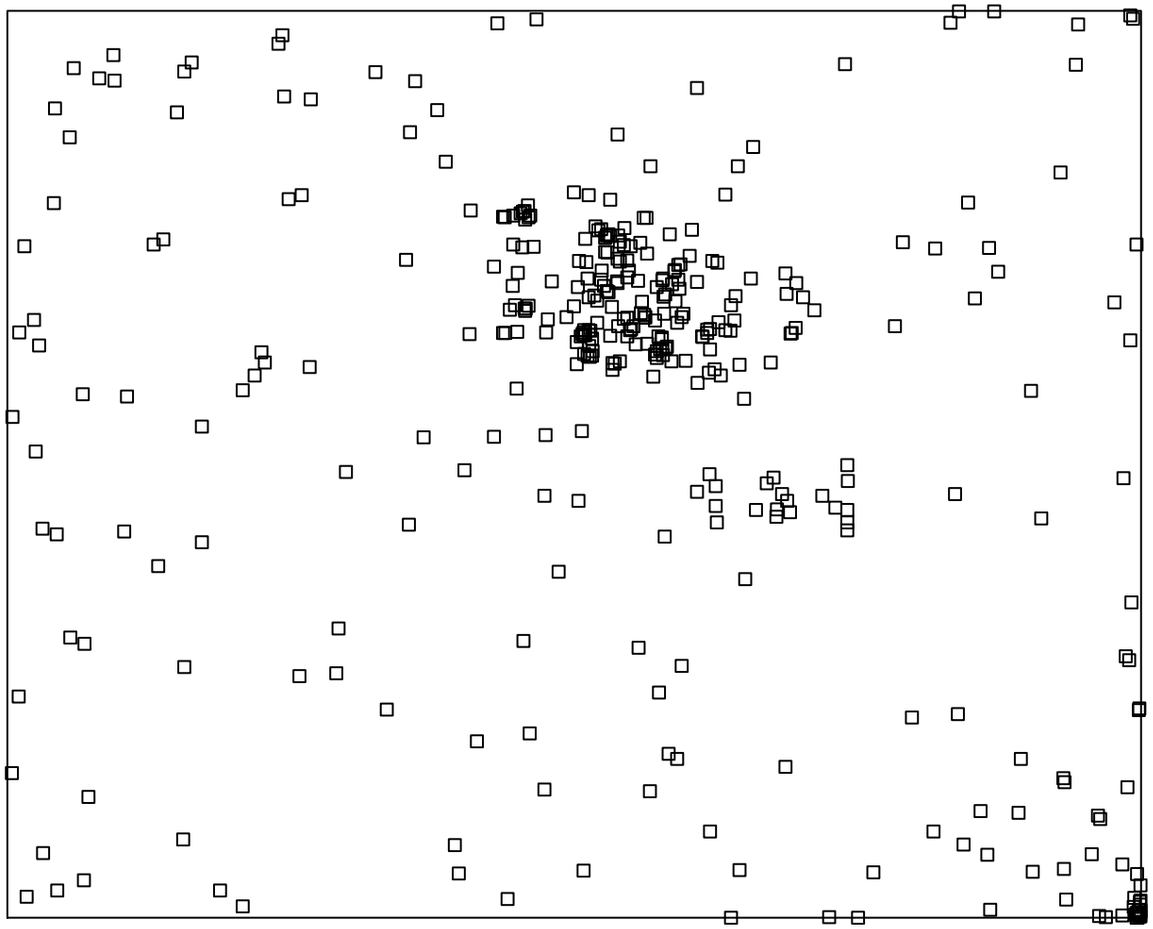

Density based thresholding (Step 2)

Remove areas with local density above threshold (medial +1.5 IQR)

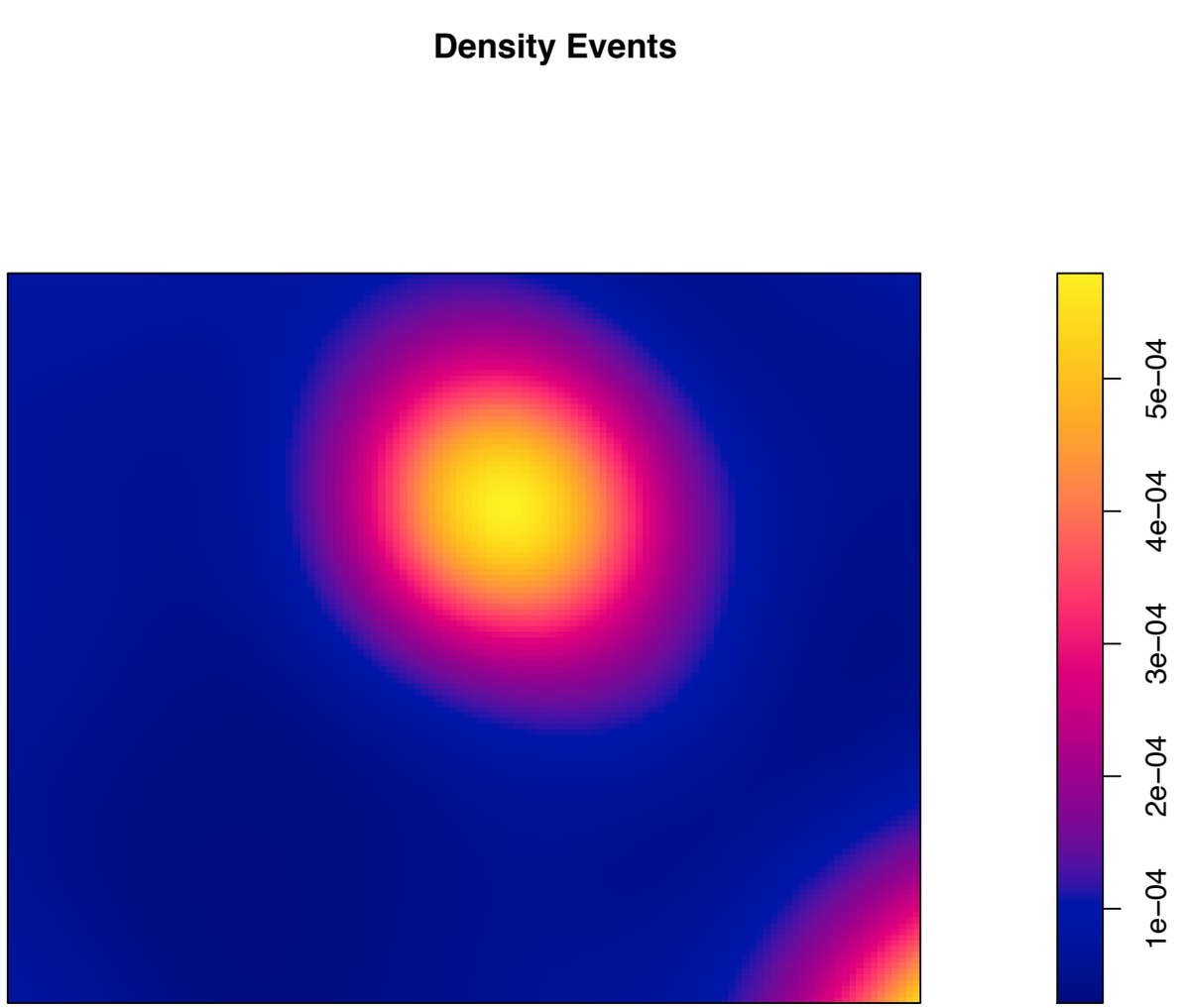

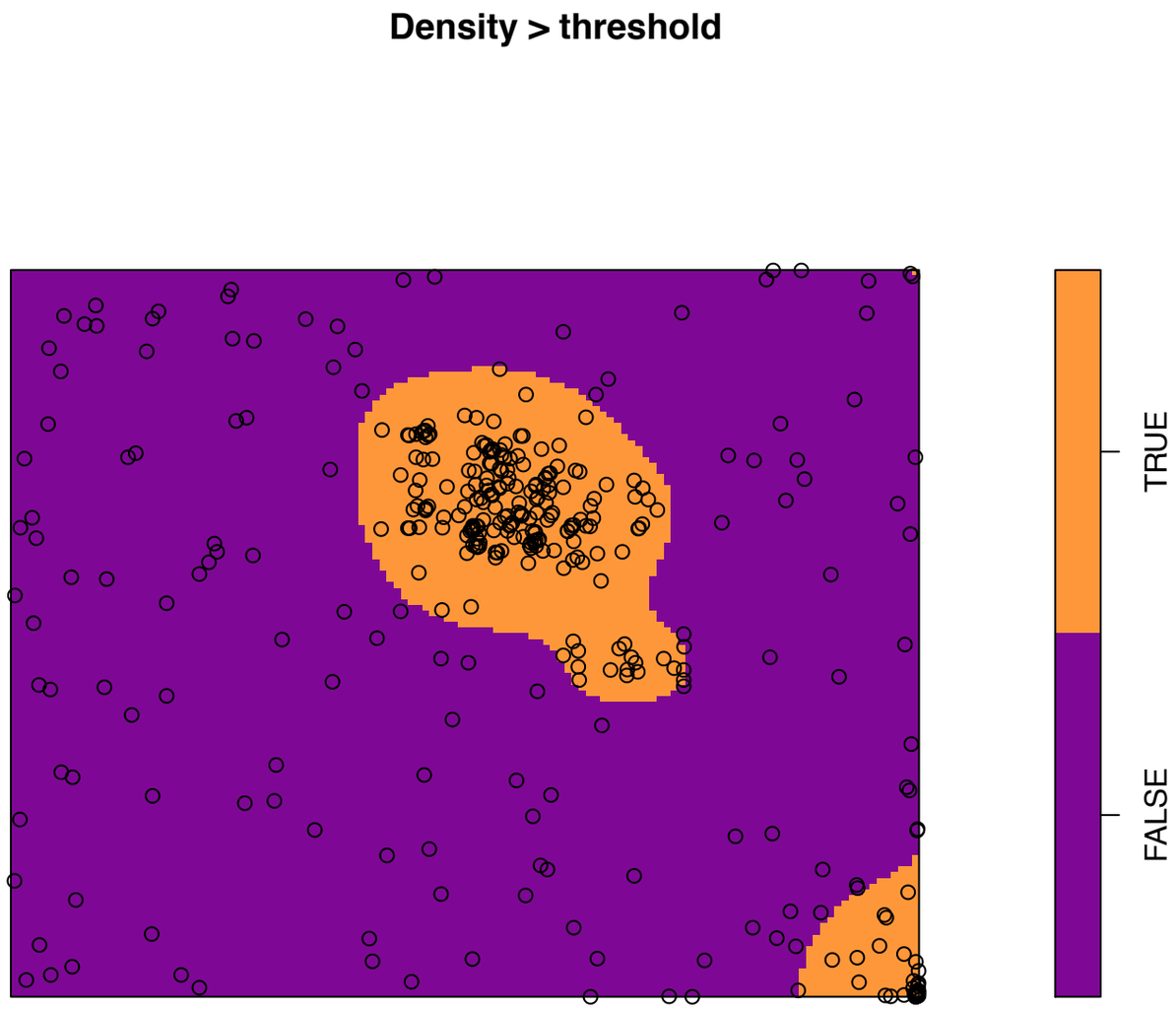

After modification: K-function

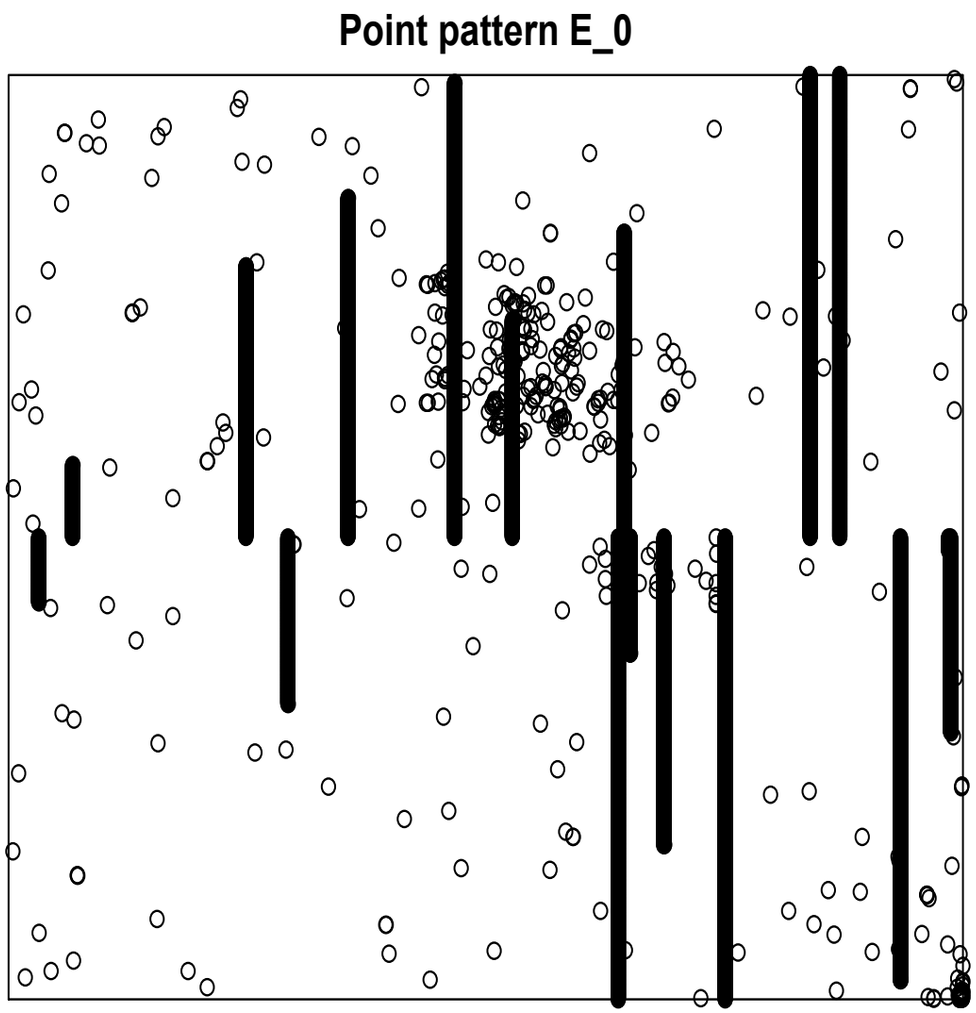

Excluding lines and area with high density

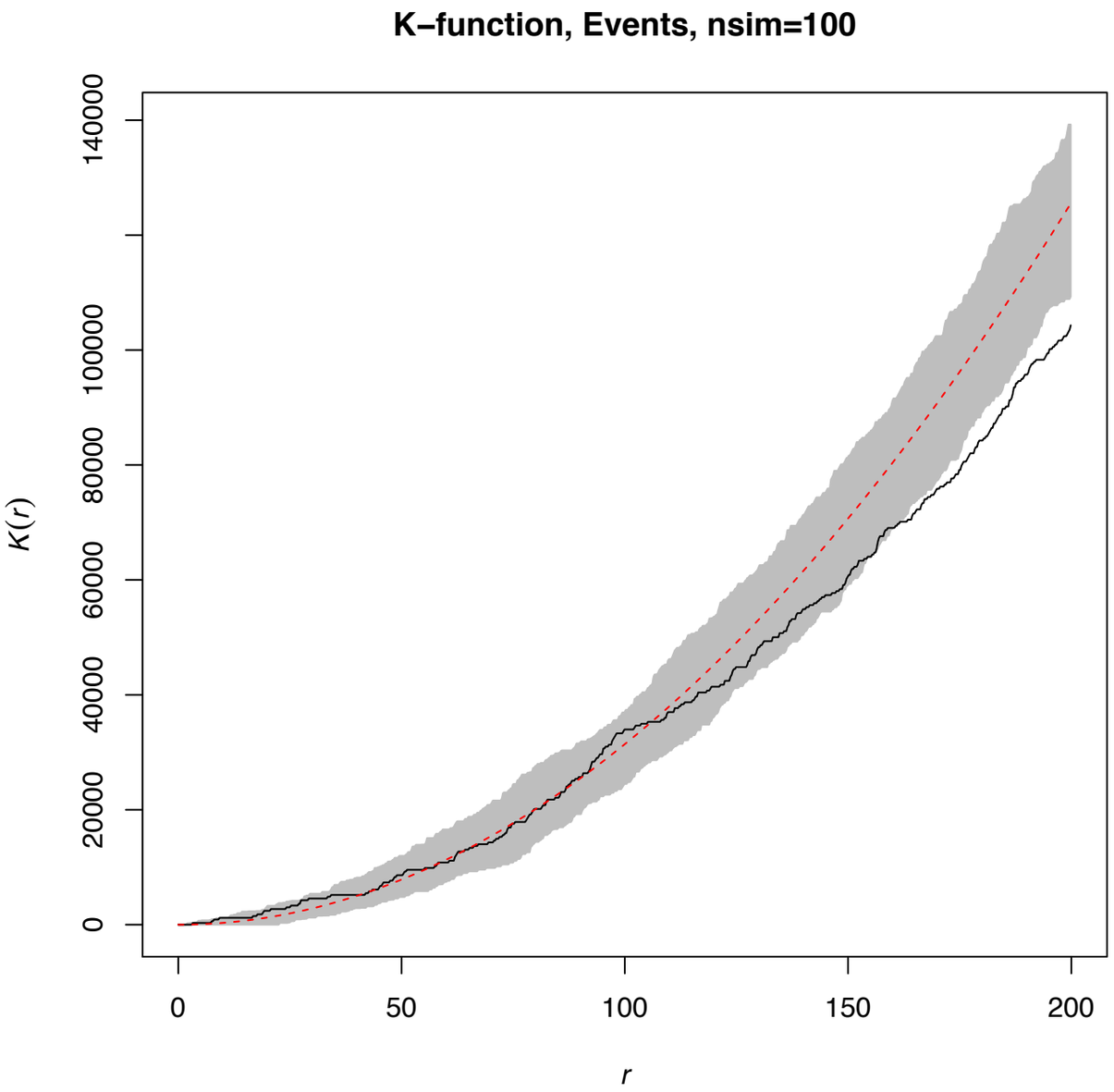

Before modification: G-function

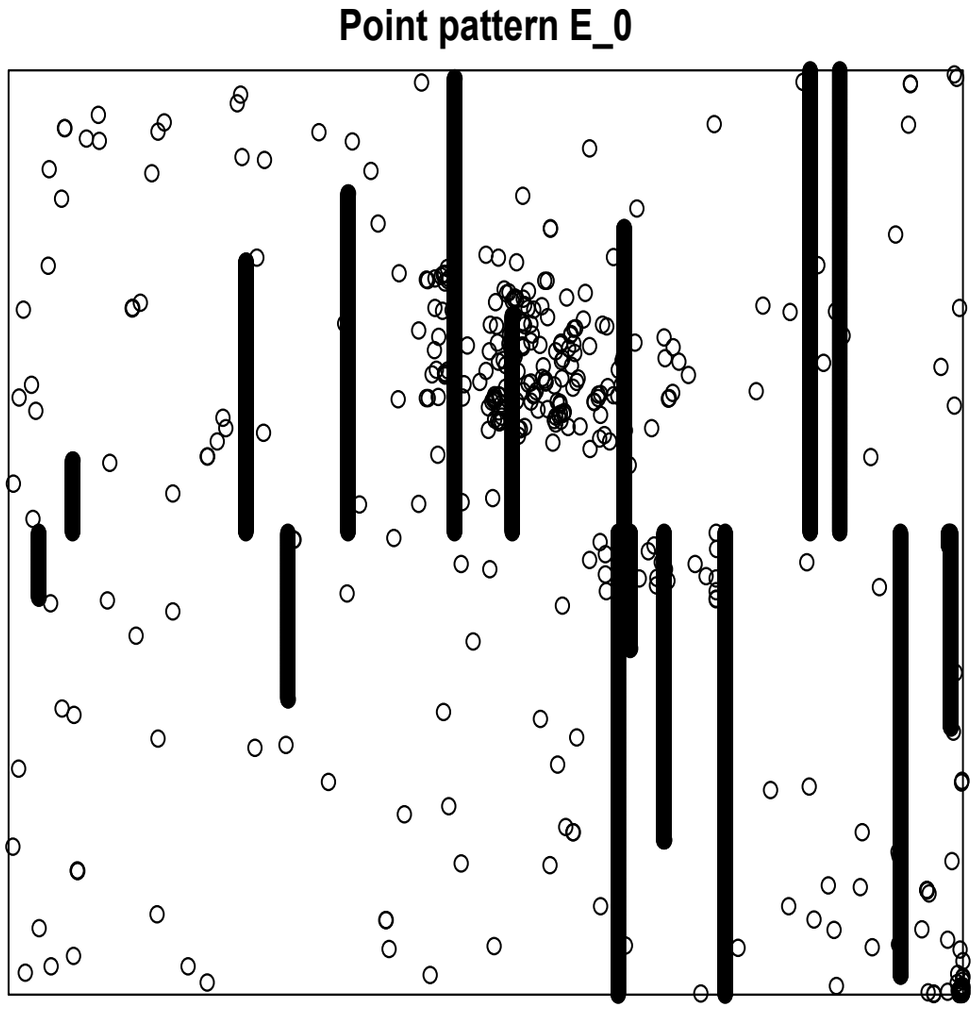

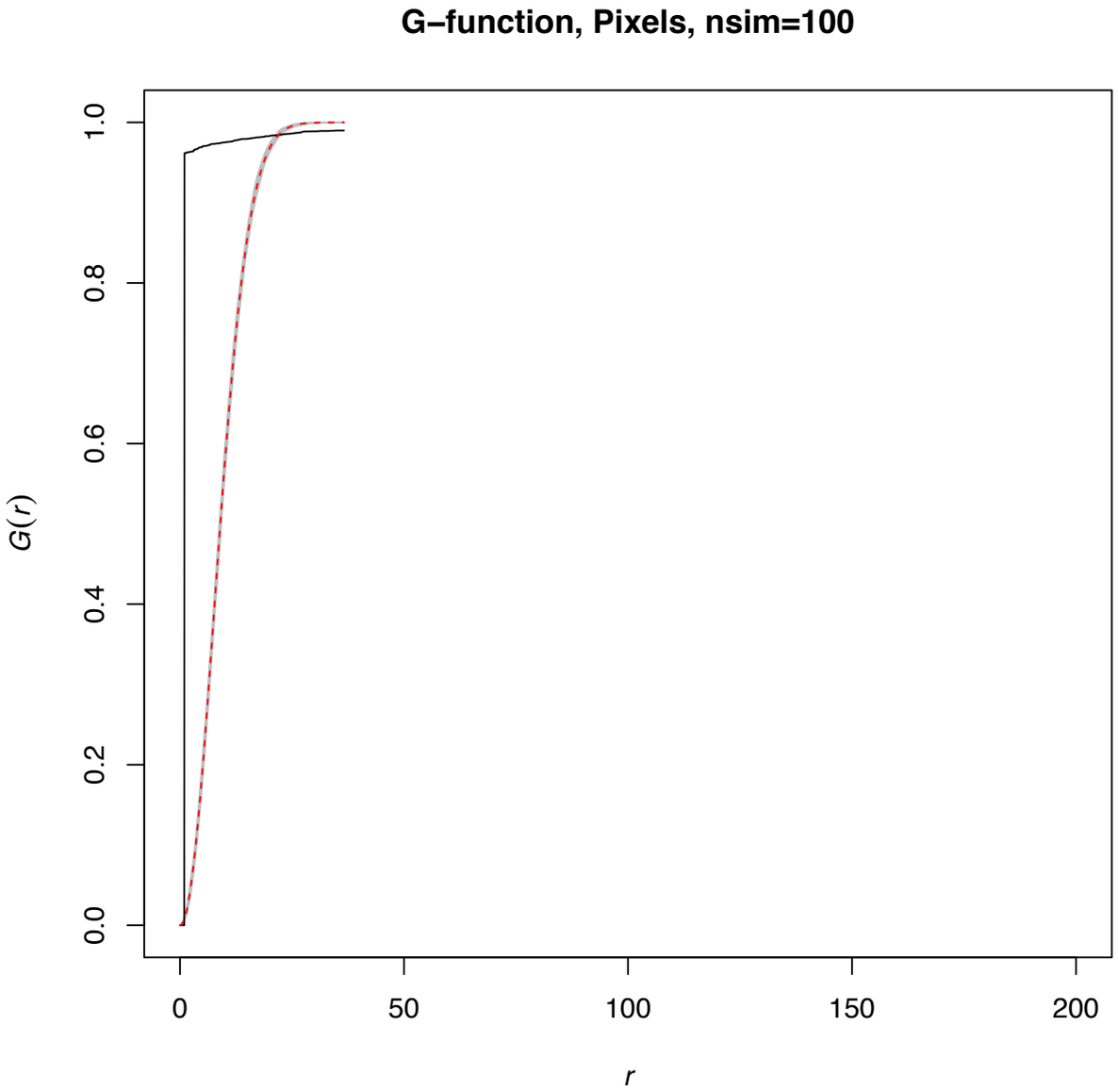

After modification: G-function

Excluding lines and area with high density

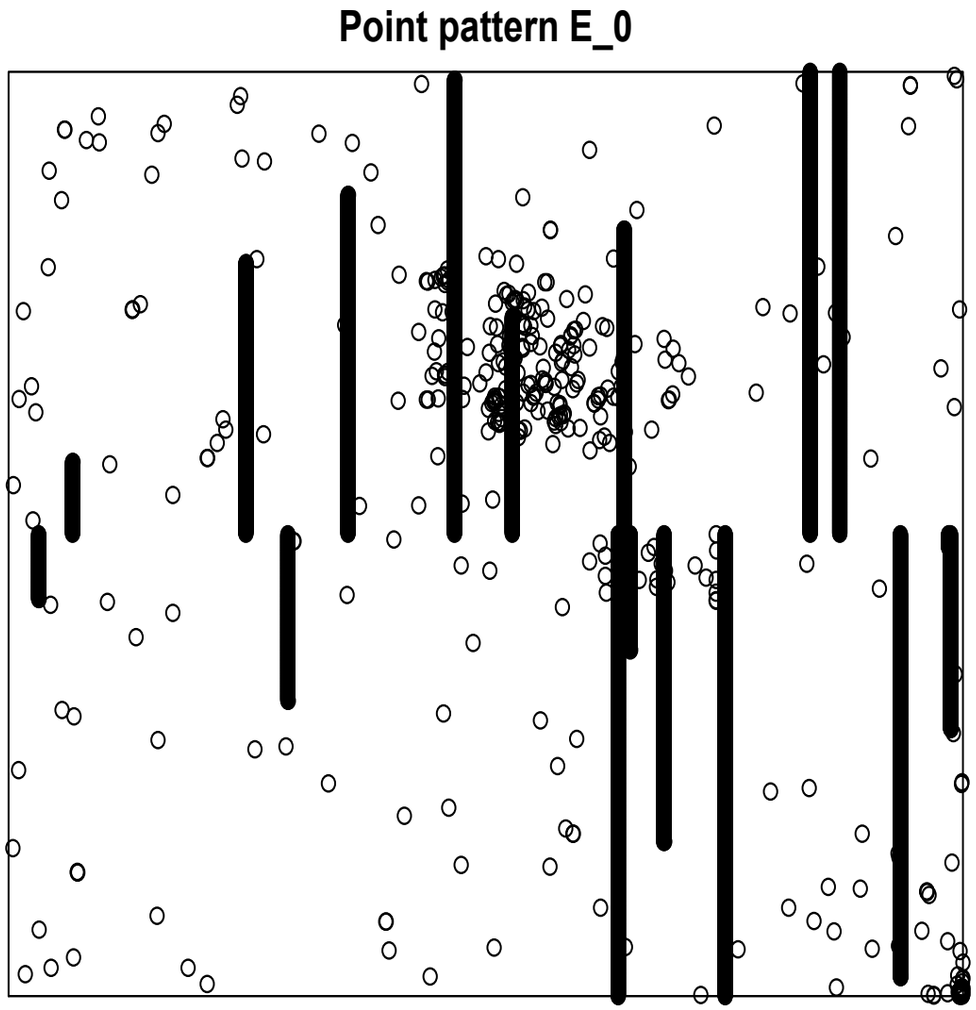

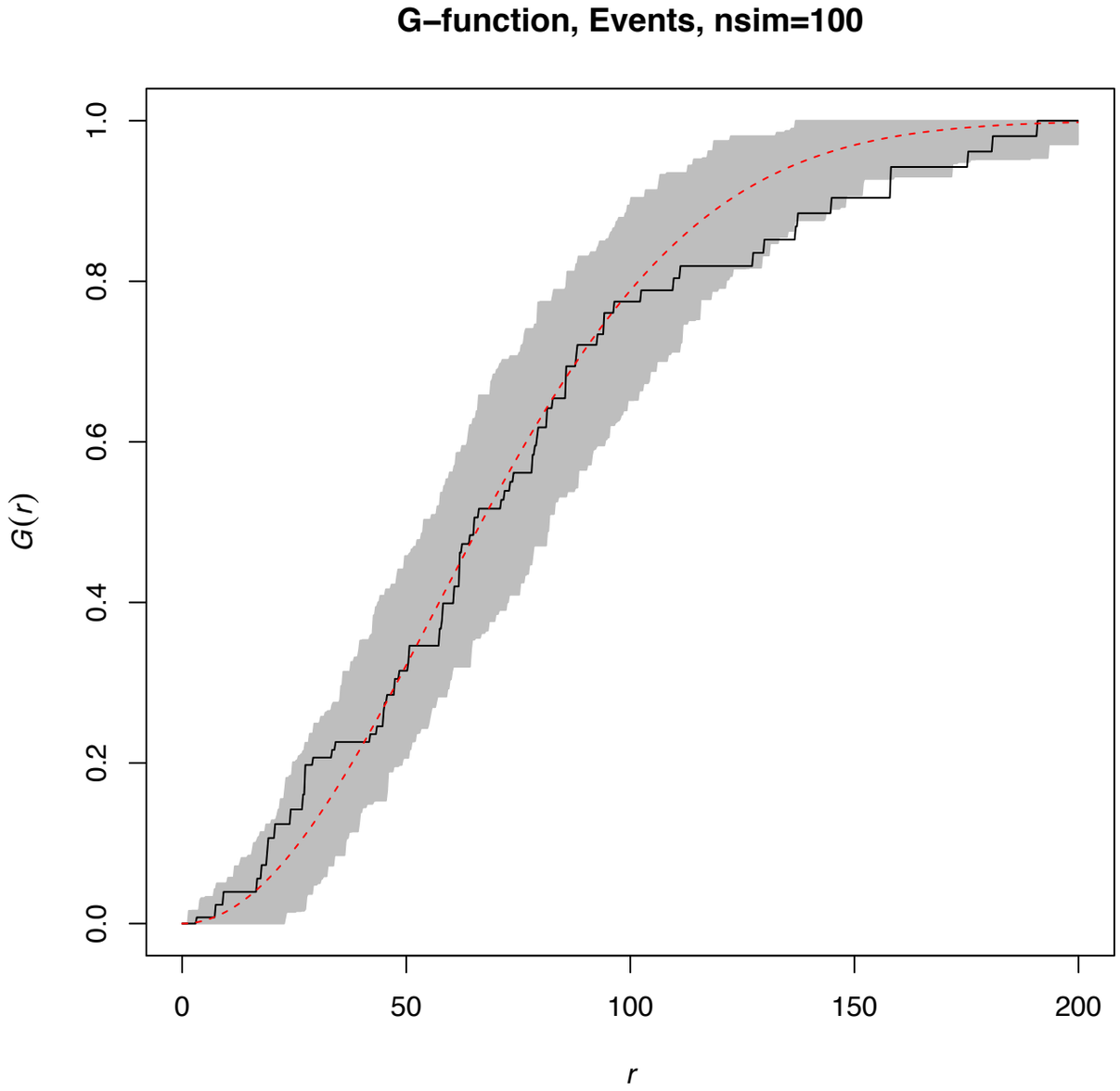

Spatial statistics for detector QA

- Transforming pixel based model into event based model makes damage independent of pixel resolution
- Fitting density allows to identify poor quality regions (patches with high dead pixels density)
- Remaining area CSR means no “special causes of poor quality” (see W. Shewhart)
- Density in remaining area gives global quality score for the detector

Software project with the Alan Turing Institute

Objectives:

Web application "DetectorChecker"

- Feedback about state of detector through pixel damage analysis
- Detector data repository

Seed funded project:

- Working with Turing Research Software Engineer Group
- *DetectorChecker* R package for statistical analysis of pixel damage in CT scanners available at https://github.com/alan-turing-institute/DetectorChecker
- *DetectorCheckerWebApp* for useful initial graphical/analysis, available at https://detectorchecker.azurewebsites.net
- Facility to upload data in different formats (crowd sourcing)

Brettschneider et al., (2020). DetectorChecker: analyzing patterns of defects in detector screens. Journal of Open Source Software, 5(56), 2474

Microtubules locations as point patterns

Stephen Royle's Lab (Centre for Mechanochemical Cell Biology) asks:
What is the role of TACC3 protein for the structure of microtubules within K-fibres and mesh?

Experiment: Overexpression of TACC3 through treatment versus control.

Data: Microscopic images collected in planes perpendicular to the fibre axes.

Perpendicular view

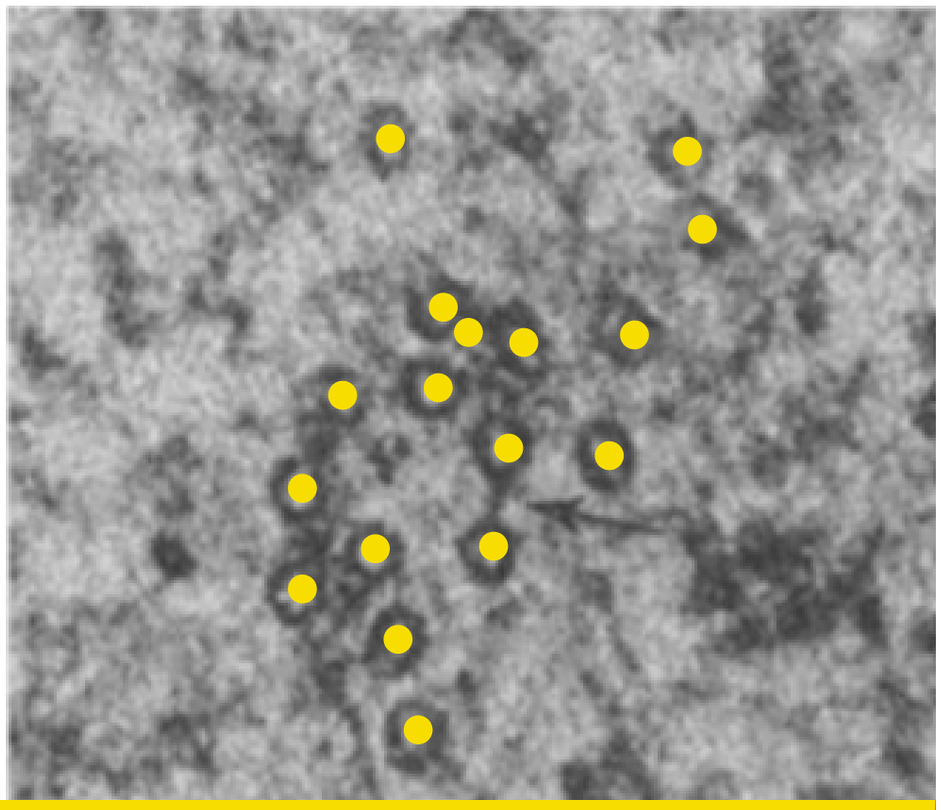

Model: locations as point pattern

Parallel

Mesh

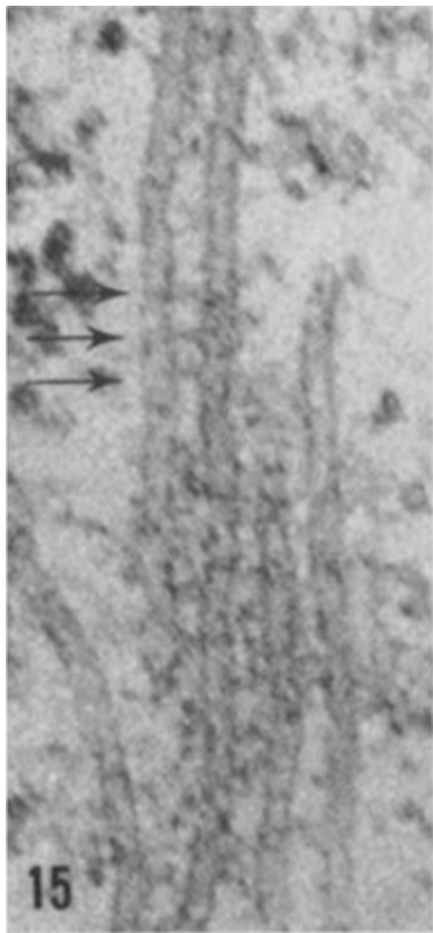

Test statistics based on basic observations

Pattern size test statistic:

$$\delta_N(I) = \frac{1}{|I_0|}\sum_{i\in I_0} n(\underline{x}^i) - \frac{1}{|I_1|}\sum_{i\in I_1} n(\underline{x}^i)$$

Observation window statistic:

$$\delta_W(I) = \frac{1}{|I_0|}\sum_{i\in I_0} |W^i| - \frac{1}{|I_1|}\sum_{i\in I_1} |W^i|$$

Intensity test statistic:

$$\sum_{i\in I_0} \omega_0(\underline{x}^i)\hat{\rho}(\underline{x}^i) - \sum_{i\in I_1} \omega_1(\underline{x}^i)\hat{\rho}(\underline{x}^i)$$

where $\delta_\rho(I)$ denotes unweighted case using $\omega_k(\underline{x}^i) = 1/|I_k|$ $(k = 0, 1)$

$\delta_{\rho,\omega}(I)$ denotes weighted case using $\omega_k(\underline{x}^i) = n(\underline{x}^i) \Big/ \sum_{j\in I_k} n(\underline{x}^j)$ $(k = 0, 1)$

Test statistics based on nearest neighbours

Mean nearest neighbour test statistic:

$$\delta_{\mathrm{nnd}}(I) = \sum_{i \in I_0} \omega_0(\underline{x}^i)\overline{\mathrm{nnd}}(\underline{x}^i) - \sum_{i \in I_1} \omega_1(\underline{x}^i)\overline{\mathrm{nnd}}(\underline{x}^i)$$

Unweighted and weighted versions as above.

Further work includes mean minimum spanning test statistics.

Test statistics based on G-functions

Estimated nearest neighbour functions averaged
over the collection of point patterns $\underline{x}^J$ with weights ω_J as above:

$$\hat{G}(\underline{x}^J, r) = \sum_{i \in J} \omega_J(\underline{x}^i) \hat{G}(\underline{x}^i, r)$$

Nearest neighbour distribution test statistic statistics:

$$\delta_{G,1}(I) = ||\hat{G}(\underline{x}^{I_0}, r) - \hat{G}(\underline{x}^{I_1}, r)||_1 = \int_0^\infty |\hat{G}(\underline{x}^{I_0}, r) - \hat{G}(\underline{x}^{I_1}, r)| dr$$

$$\delta_{G,\infty}(I) = ||\hat{G}(\underline{x}^{I_0}, r) - \hat{G}(\underline{x}^{(I_1}, r)||_\infty = \sup_r |\hat{G}(\underline{x}^{I_0}, r) - \hat{G}(\underline{x}^{I_1}, r)|$$

For comparison of $\hat{G}(\underline{x}^{I_0}, r)$ and $\hat{G}(\underline{x}^{I_1}, r)$
across the range of distances $r > 0$.

Also, scaled neighbourhood count test statistic (Diggle 2000).

Significance quantification

- Based on permutation tests (nonparametric)
- Need exchangeability under the Null under suitable set of operations
- Statistics under permutations are identically distributed
- p-values are uniformly distributed (test e.g. with KS)
- Exact or approximate (subset of operations)

Operations $\Gamma = \{\gamma_0, \gamma_1, \ldots, \gamma_m\}$, where $\gamma_0 = \mathrm{Id}$.

p-value for two-sided test of H_0 using statistic t :

$$p = \frac{1}{m+1} \sum_{\gamma \in \Gamma} 1_{\{|t(\gamma x)| \geq |t(\gamma_0 x)|\}}$$

Γ : random subsets of the symmetric group S_I

Permuted I results in subsets $I_0^{(j)}$ and $I_1^{(j)}$ satisfying

$$I_0^{(j)} \cup I_1^{(j)} = I,\ I_0^{(j)} \cap I_1^{(j)} = \emptyset,\ |I_0^{(j)}| = |I_0|,\ |I_1^{(j)}| = |I_1|$$

Simulation study

- Homogeneous Poisson process density ρ
- Inhomogeneous Poisson process with density $\rho(x)$
- Cluster point pattern generated by rejection sampling algorithm

Data: d, W

Result: Point pattern $\underline{x}$ on W with nearest neighbour distances $\{d_1\} \cup d$

$x_1 \leftarrow$ centre of W;

for i *in* $1:n$ **do**

  repeat

    $j \sim \text{Uniform}\{1, \ldots, i\}$;

    $\theta \sim \text{Uniform}[0, 2\pi]$;

    $x_{i+1} \leftarrow x_j + d_i(\cos\theta, \sin\theta)$;

  until $\min_{k \in \{1,2,\ldots,i\}} ||x_{i+1} - x_k|| \geq d_i$ *and* $x_{i+1} \in W$;

end

$\underline{x} \leftarrow (x_1, x_2, \ldots, x_{n+1})$;

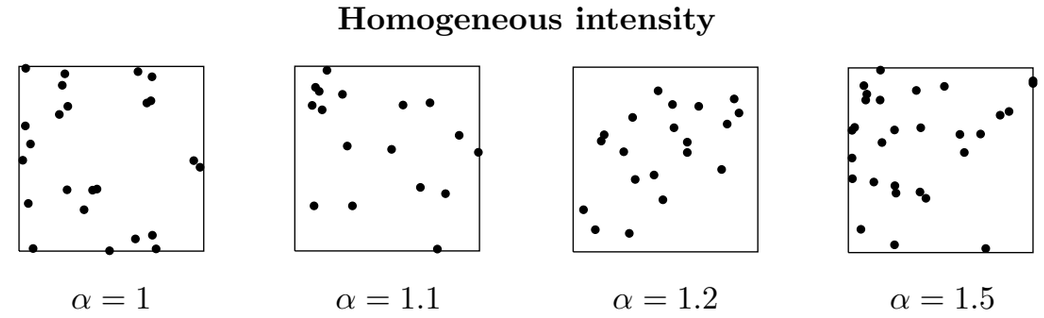

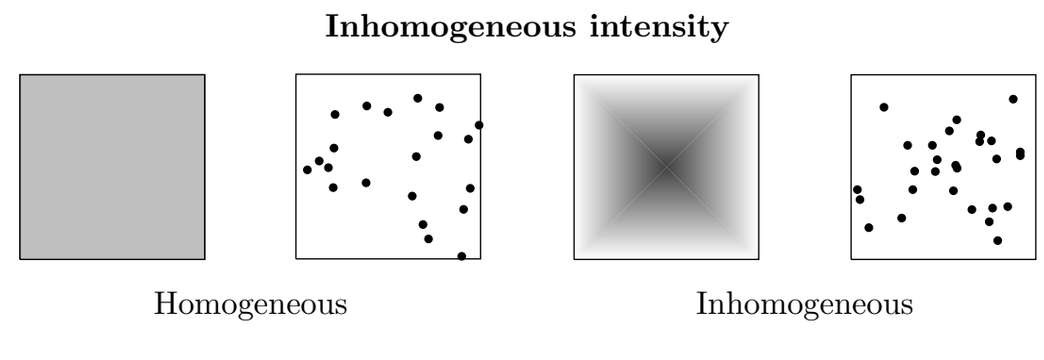

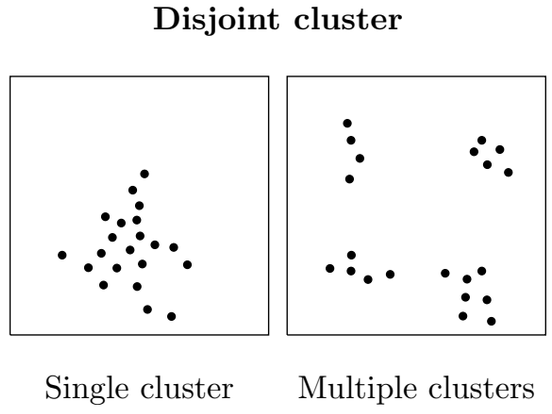

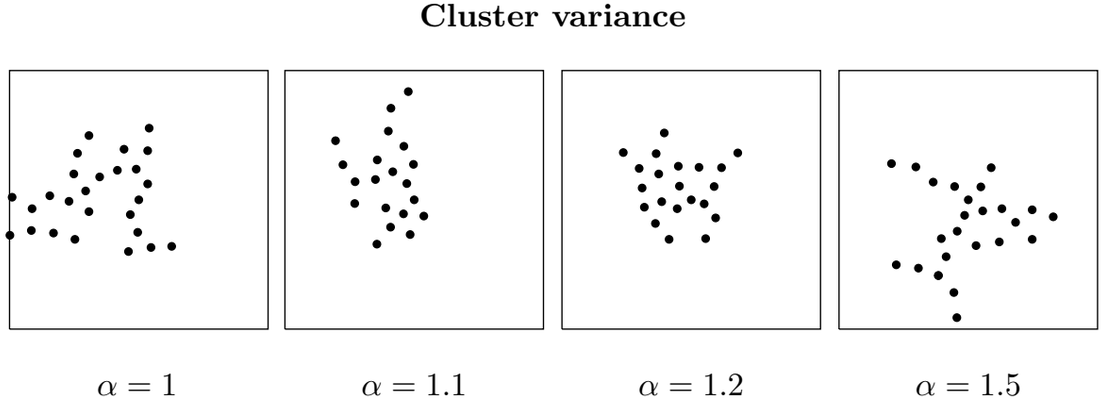

Study I: Microtubules

Stephen Royle's Lab (Centre for Mechanochemical Cell Biology):

What is the role of the TACC3 protein for the structure of microtubules within K-fibres and mesh?

Experiment:

Overexpression of TACC3 through treatment versus control.

Microscopic images collected in planes perpendicular to the fibre axes.

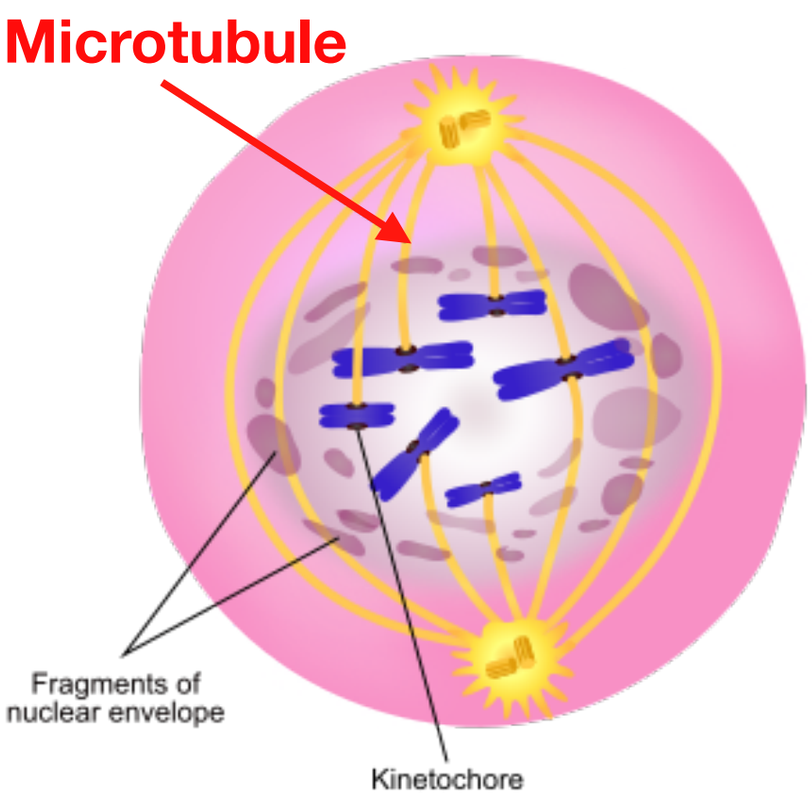

Perpendicular to the microtubule axis

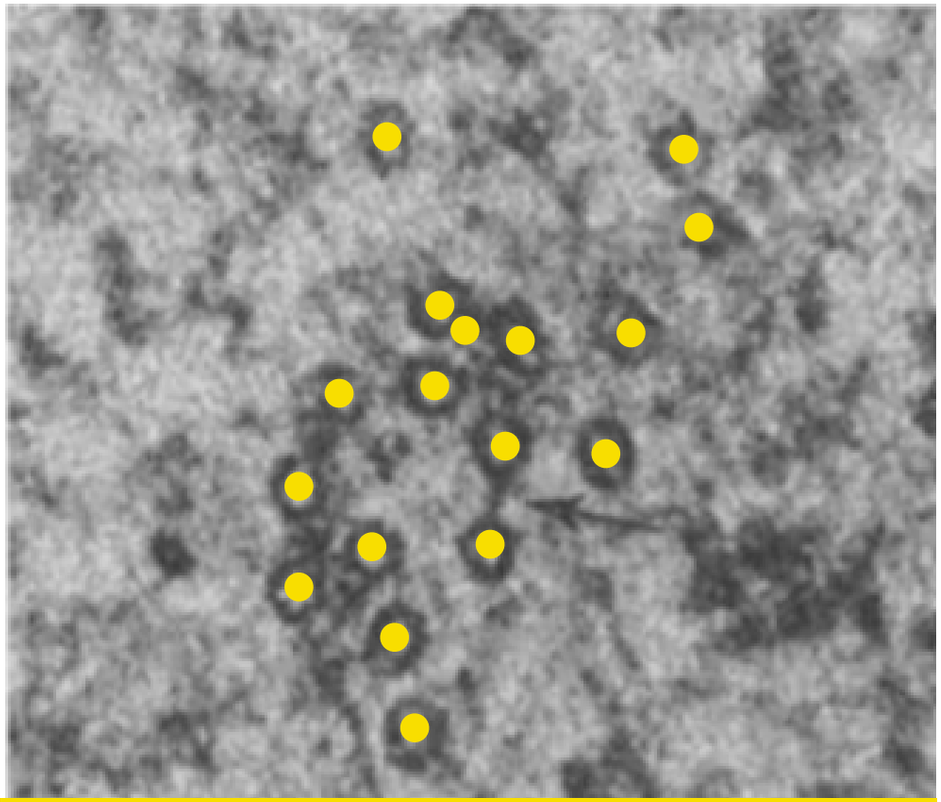

Model locations as point pattern

Parallel showing mesh

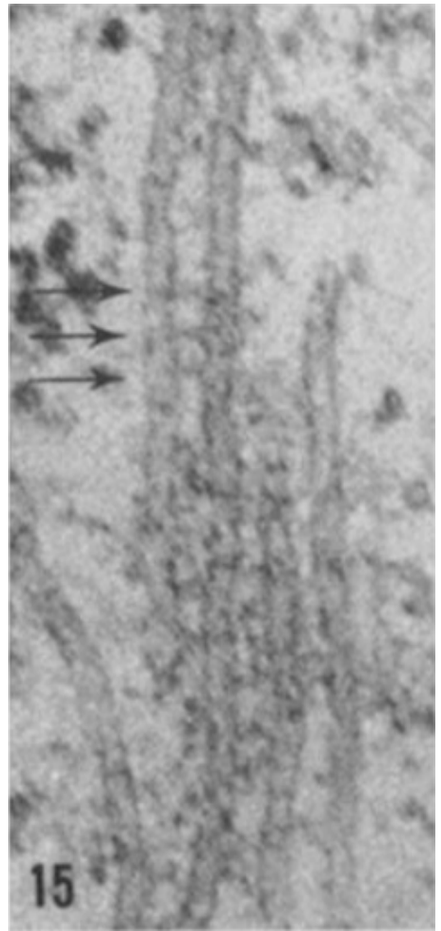

Study I: Microtubules - mathematical model

Data:

Microscopic images of treatment (n=37) versus control (n=26)

Observation window surrogate for cross sectional area of K-fibres

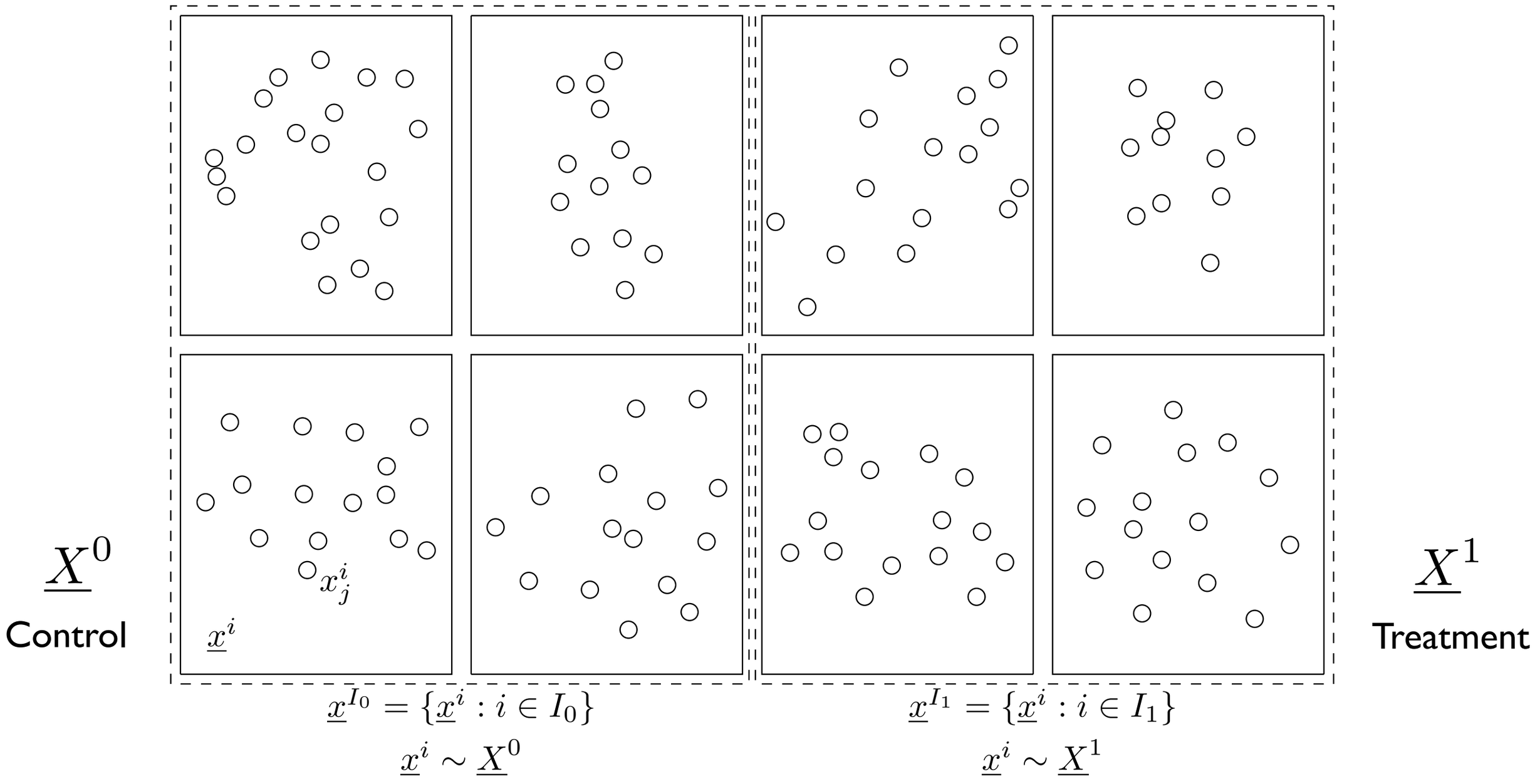

EDA: First order statistics

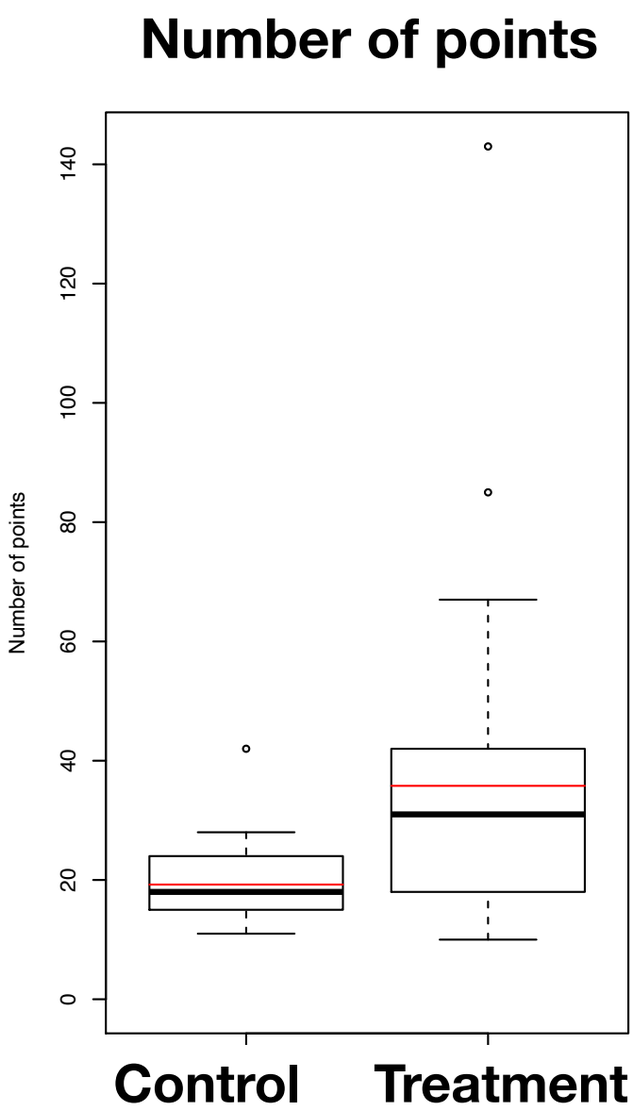

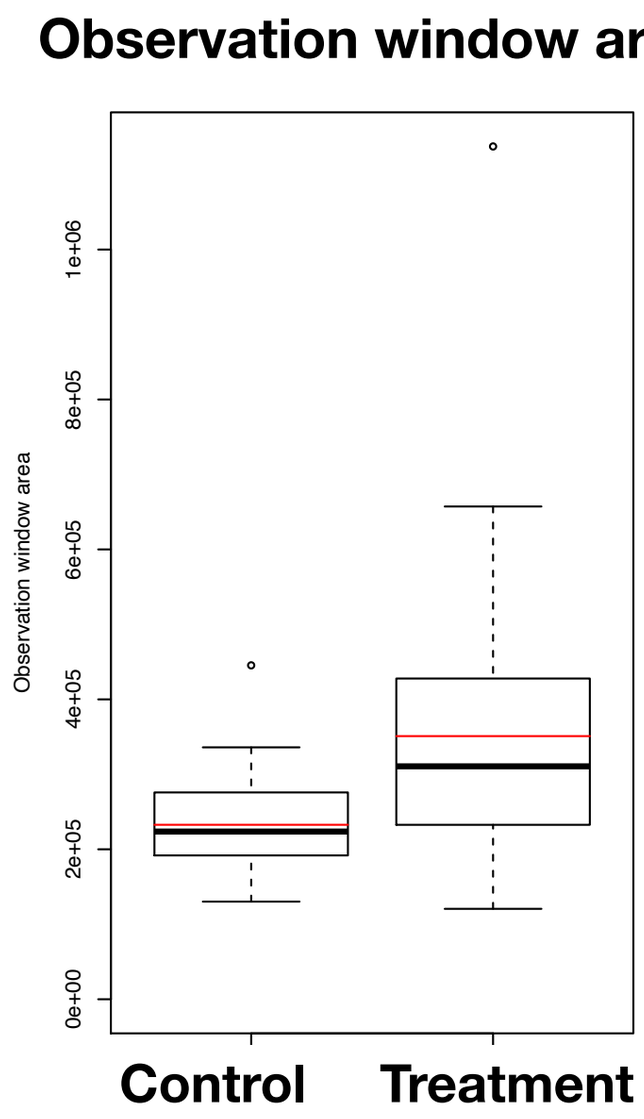

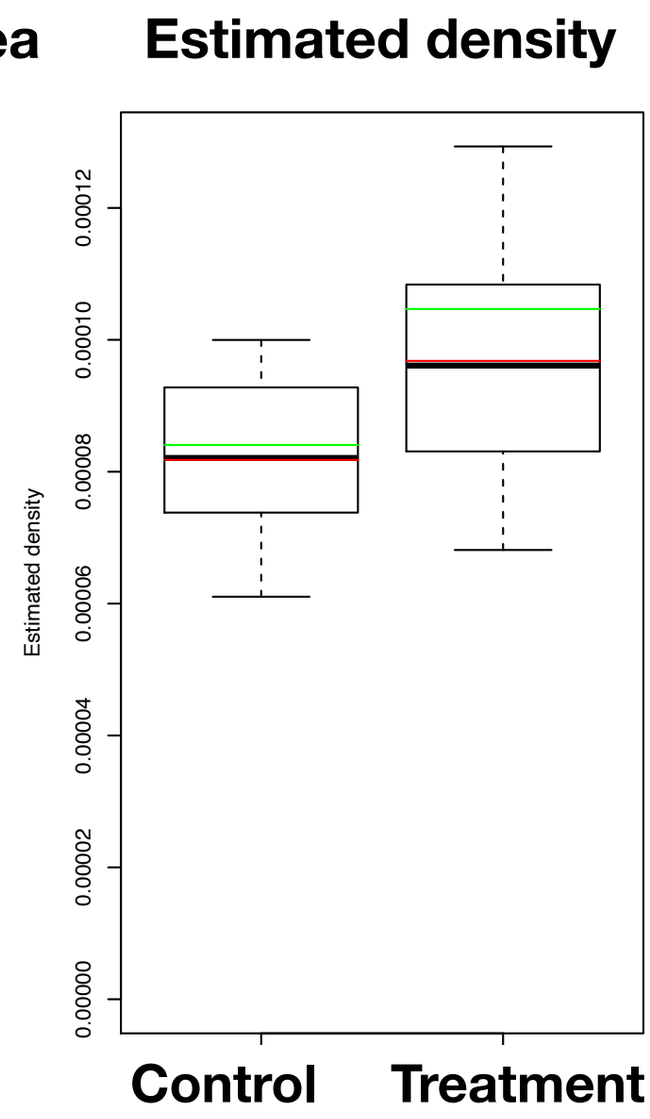

mean
weighted mean

- All means/medians are greater for treatment
- Treated K-fibers are made up of a greater number of microtubules which are more closely separated within thicker K-fibers
- Weighted mean densities greater than unweighted means densities (i.e. K-fibers with greater numbers of microtubules are more tightly packed

EDA: Second order statistics

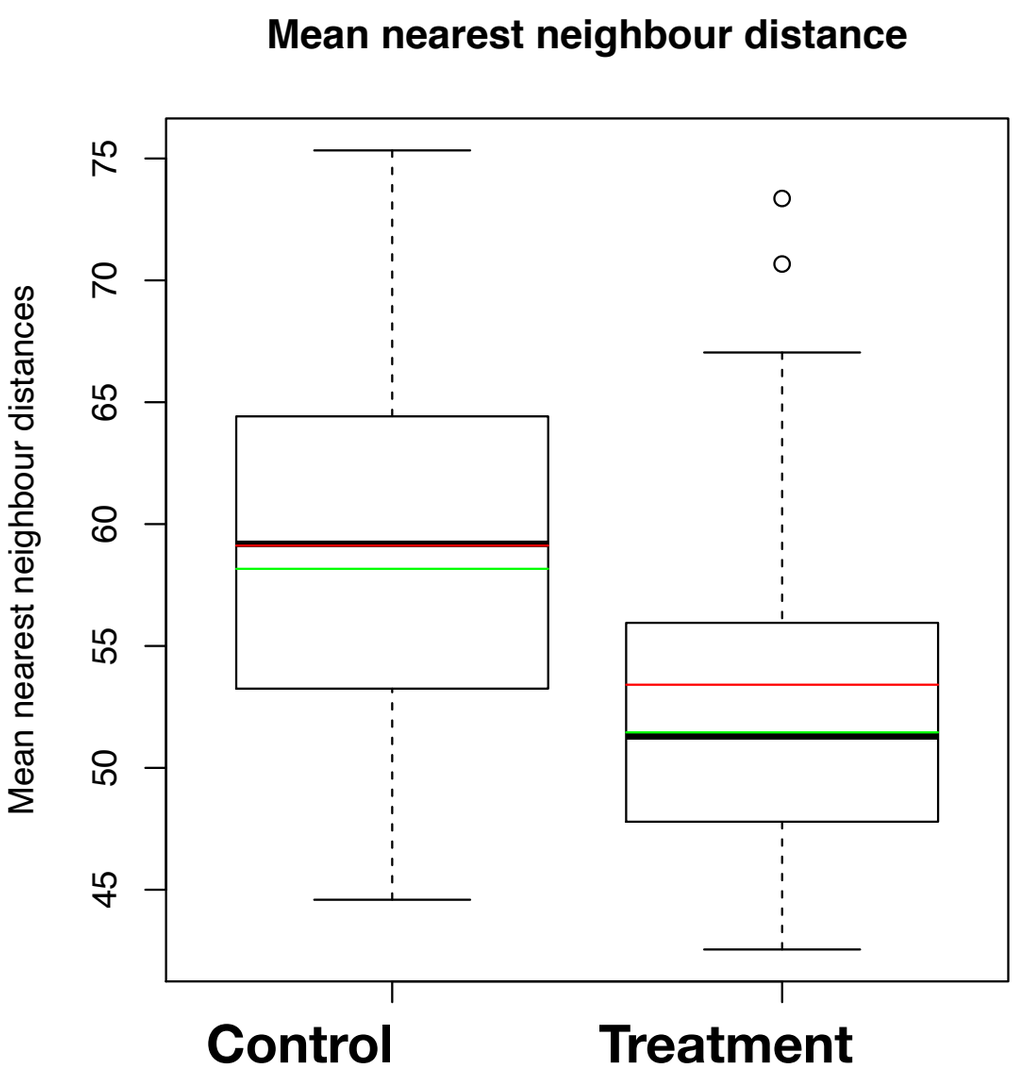

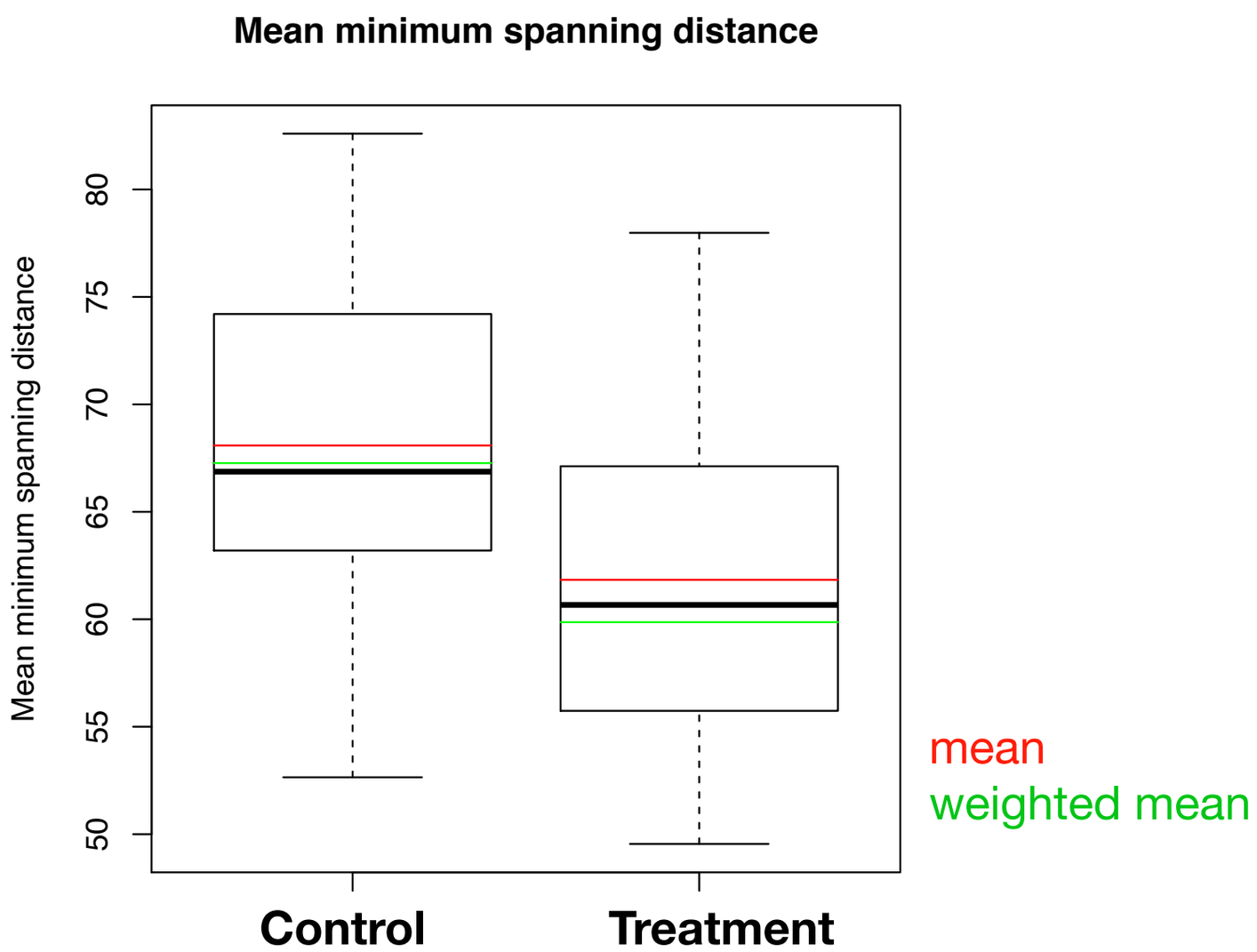

- In each case the average separation distance is reduced for treatment observations
- Weighted means smaller than unweighted means (i.e. K-fiber with more microtubules are more tightly packed).

EDA: Spatial functions

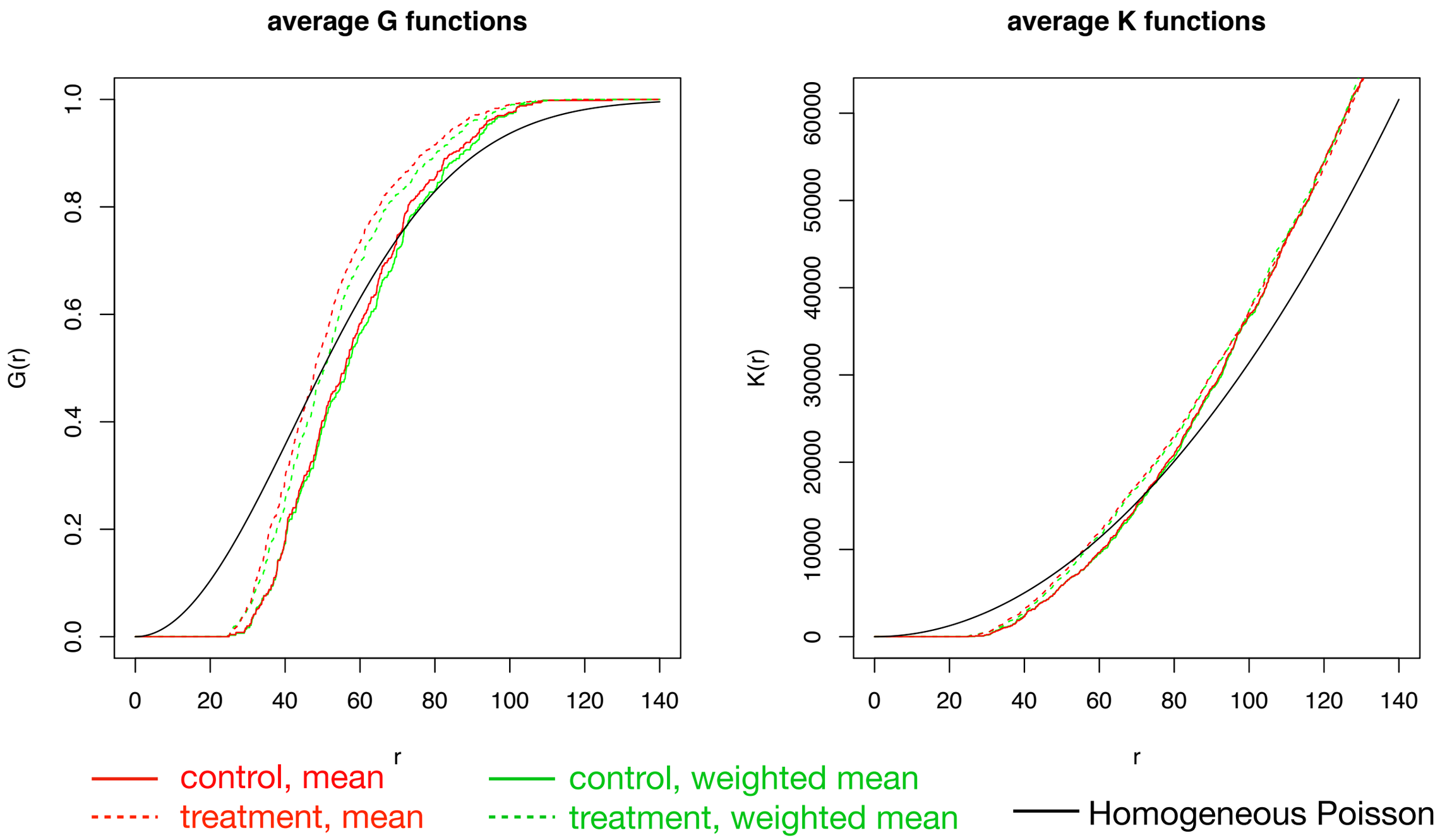

- Some evidence of clustering at larger length scales
- Effect of limitation of nnd in [25,105]
- Difference between weighted mean and unweighted mean negligible

Test statistics

Observations of exploratory analysis can be confirmed by formal testing.
All proposed test statistics show significant results:

δ_N	0.0005	δ_{nnd}	0.0057	δ_K	0.1092	δ_{EFT}	0.0011
δ_W	0.0018	$\delta_{\text{nnd},\omega}$	0.0005	$\delta_{G,1}$	0.0061	$\delta_{EFT,\omega}$	0.0005
δ_ρ	0.0001	δ_{msd}	0.0019	$\delta_{G,1,\omega}$	0.0005		
$\delta_{\rho,\omega}$	0.0002	$\delta_{\text{msd},\omega}$	0.0005	$\delta_{G,\infty}$	0.0087		
				$\delta_{G,\infty,\omega}$	0.0013		

Results remain significant after multiple testing adjustment of critical p-value (using Bonferroni).

What did we find?

- Microtubules are **bound together** (in K-fibers, by mesh-like structure)
- TACC3 **overexpression** is **associated with an impact** on the mesh
- Detection of treatment effects not visible by eye

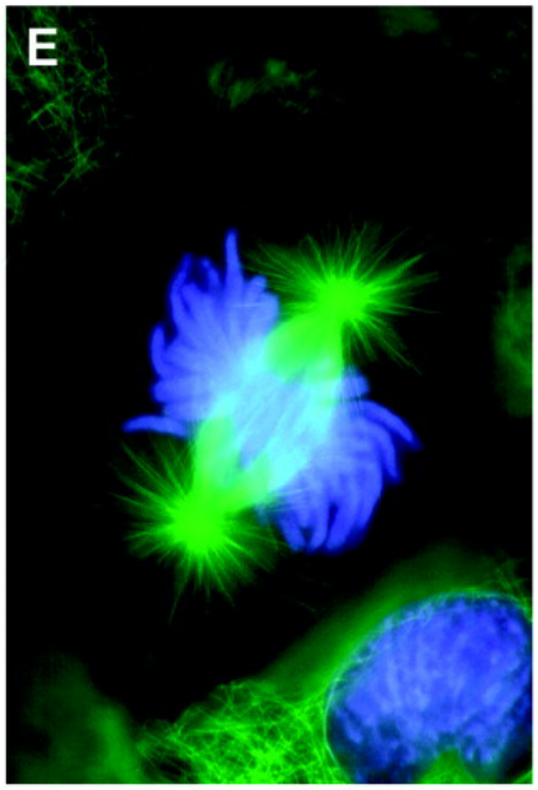

Perpendicular to the microtubule axis

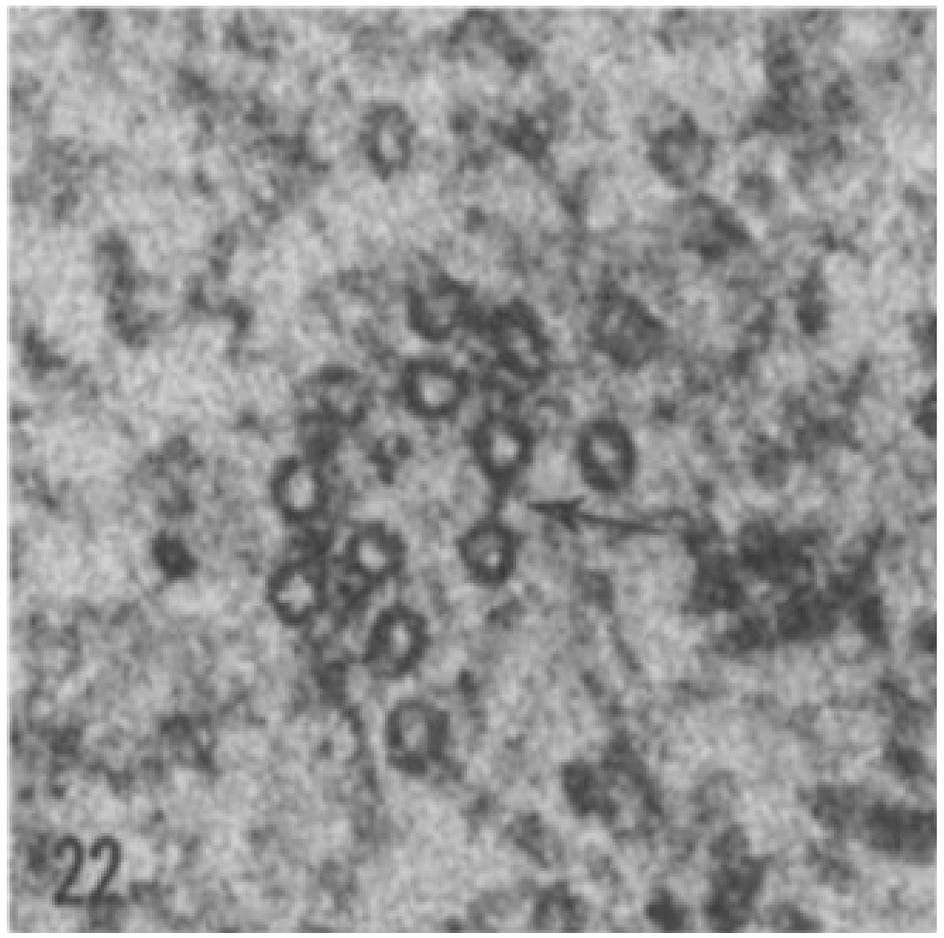

Parallel view

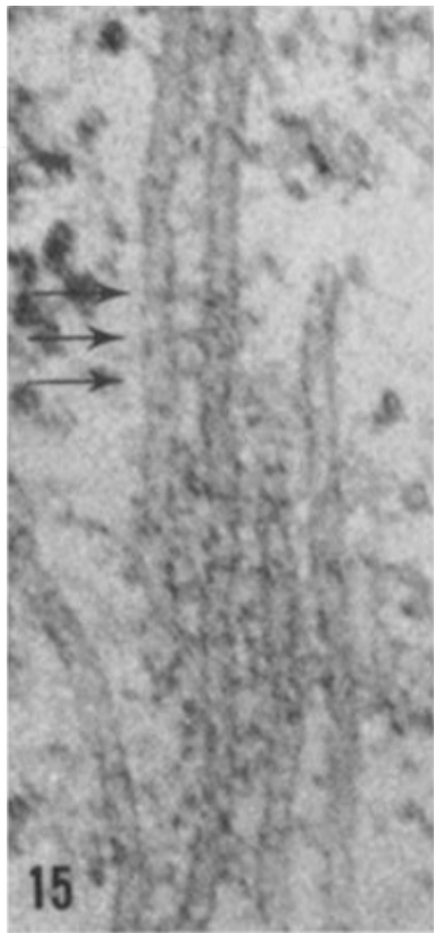

About right and wrong

What are models for? Prediction and explanation. Answering questions…

> *"Far **better an approximate answer to the right question**, which is often vague, than the exact answer to the wrong question, which can always be made precise."*
>
> John Tukey (1915-2000)
> American statistician (FFT, various statistical tests, EDA)

How good is a model?

> *"All models are wrong, some are **useful**."*
>
> George Box, FRS (1919-2013)
> English statistician (quality control, time series, design of experiments, response surfaces, Bayesian inference etc)

Rephrase "how good":

How good is it *at the task what you want it to do (prediction and/or explanation)*?

Relationship between two proteins over time

Background and questions

- Protein EB3 localises at the tip of growing microtubules during mitosis.
- Relationship between TACC3 and EB3?
- Role of the protein TACC3 during that same process?

Data

- Confocal fluorescence microscopy images collected across seven samples at a total number of between 47 and 57 time points.
- Images are collected of live cells during mitosis with TACC3 tagged with a green fluorescing protein and EB3 tagged with a red fluorescent protein.

Question that can be answered from images

Is the protein TACC3 present in the same locations as the protein EB3 during the process of mitosis?

Dependencies between bulk movement patterns

Mathematical formulation of case study question

What is the relationship between two bulk movement patterns?

Modelling

- Measure for closeness of two spatial protein distributions
- Comparing their evolution over time

Applications

- Animals e.g. predator and prey (Mitchell and Lima, 2002)
- Air particles, e.g. pollution
- Cellular structures (Chenouard 2014)

Tool: Colocalisation of proteins

Example for (traditional) visual detection of colocalisation

Colocalization in the lateral optical plane of the cytoskeletal protein **actin** with **vinculin**, a protein associated with focal adhesion and adherens junctions.

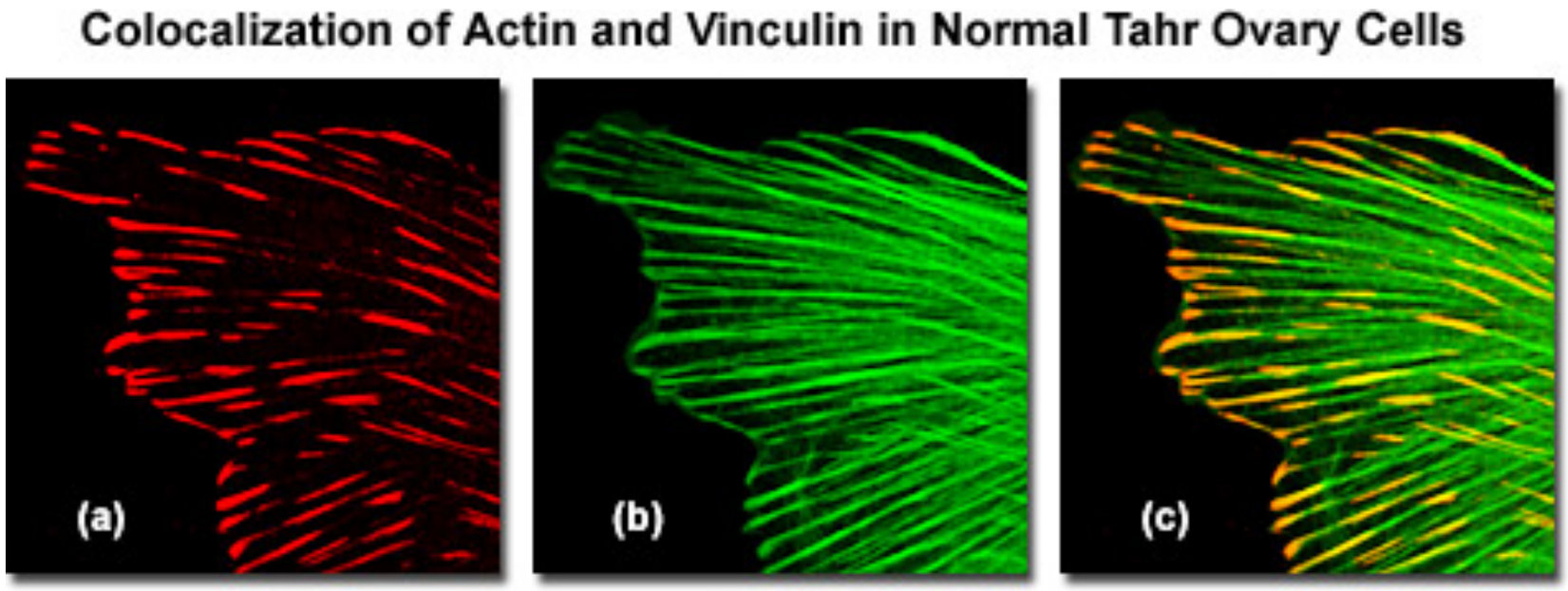

Figure 1

Applications

- Detect physical location within cell
- Uncover functions of proteins based on location
- Unravel interactions, build networks, infer function

http://www.olympusmicro.com/primer/techniques/confocal/applications/colocalization.html

Quantifying colocalisation (static)

Correlation

$$r_p = \frac{\sum_i (A_i - a)(B_i - b)}{\sqrt{\sum_i (A_i - a)^2 (B_i - b)^2}}$$

where A_i and B_i are the voxel or pixel intensities (also called grey values) of channels A and B, respectively, and a and b are the corresponding average intensities over the entire image.

- Scaling invariant
- Costes' threshold to deal with noise
- Ongoing area of research, e.g. Wang et al. (2018) for automatic segmentation

Quantifying colocalisation: Illustration

Correlation examples (simulations) for hypothetical proteins X and Y

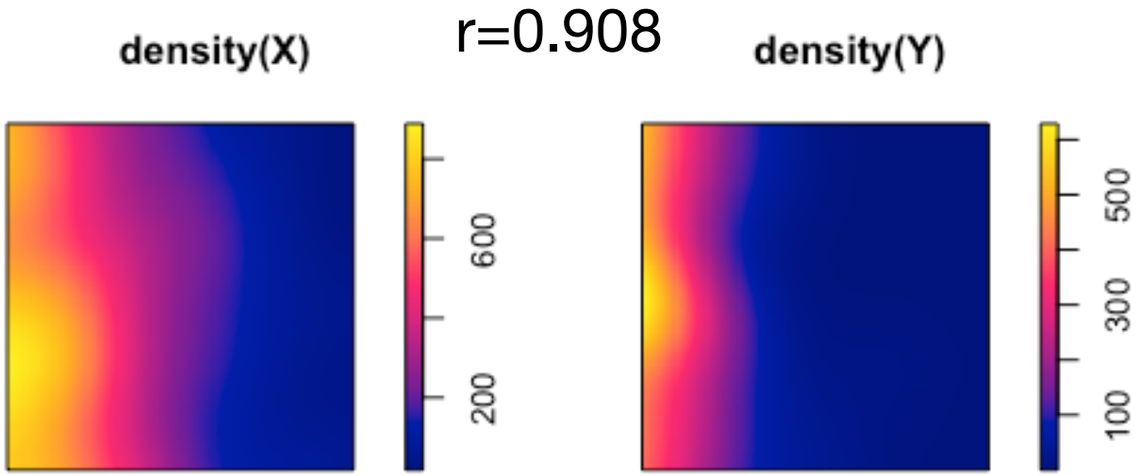

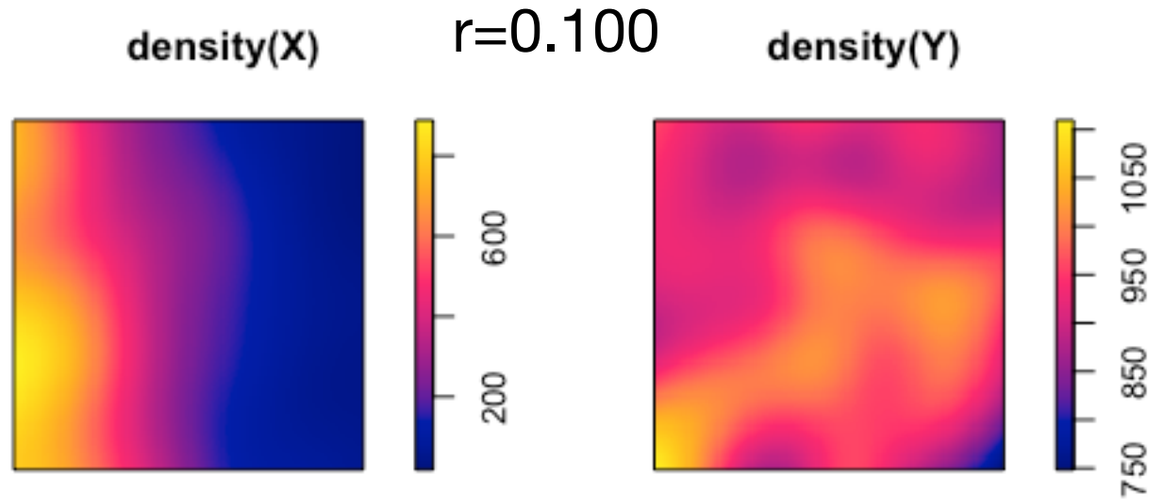

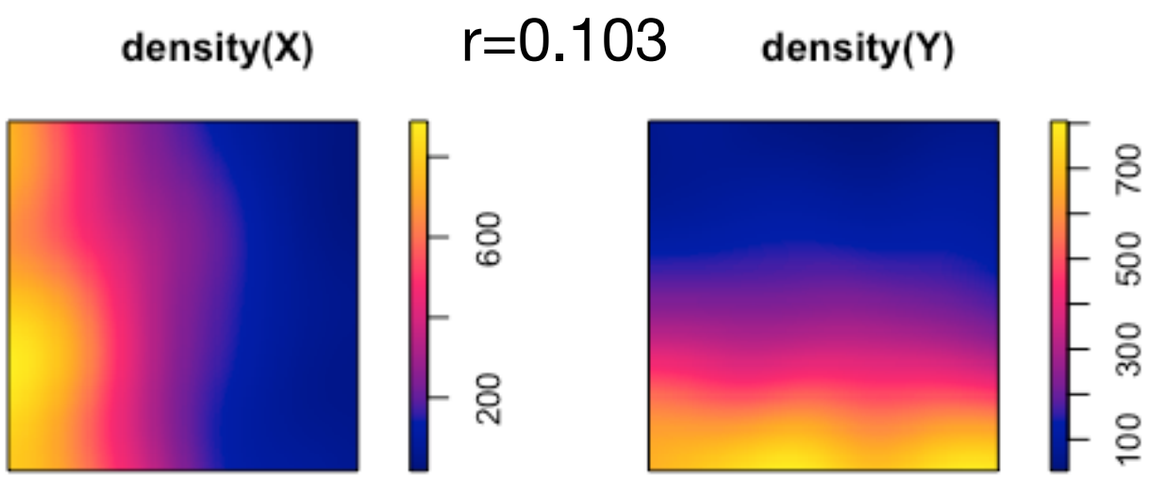

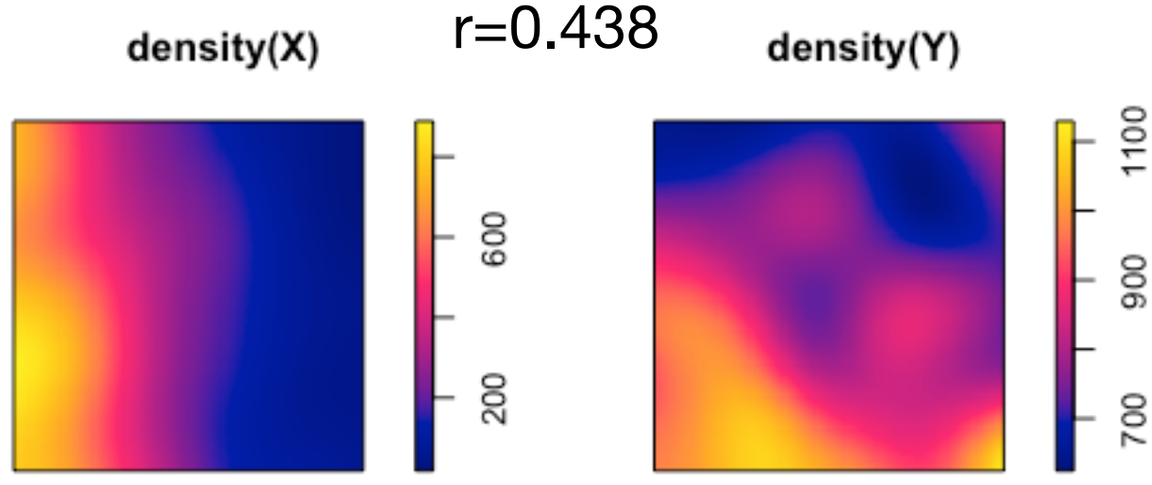

Intuitive check:
Colocalisation for consecutive time points

Colocalisation of protein distribution between consecutive time points for each sample combination of TACC3, TACC3 (vertical reflection), and EB3.

TACC3* and TACC3: only coincidental similarity expected

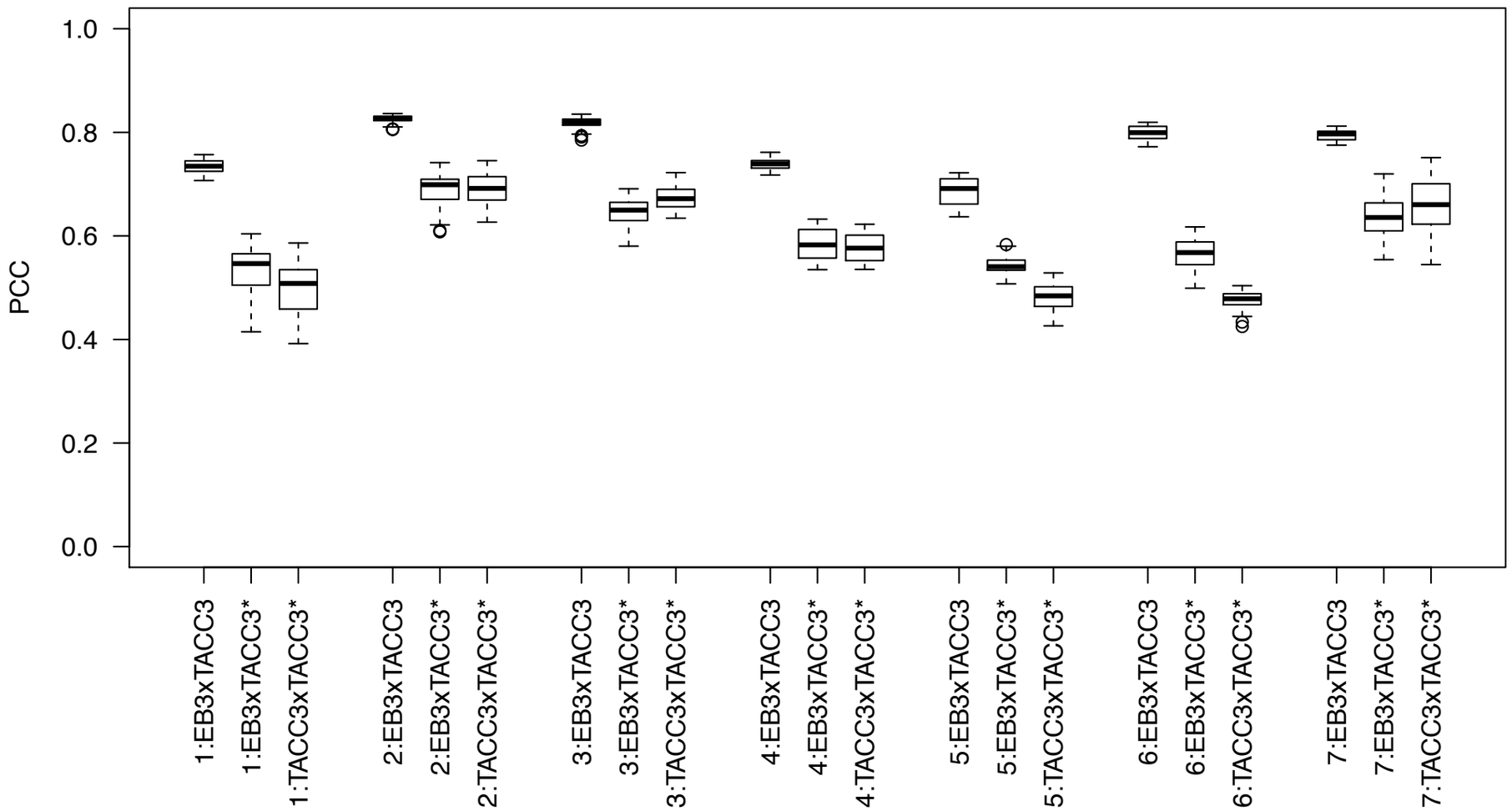

Colocalisation of EB3 with TACC3 is always higher than any of the other combinations.

Model for bulk movement patterns

Need to have a model the captures the evolution rather than individual time points.

Observed pixel intensity values $m^0(x)$ and $m^1(x)$ across ROI:

$$\Psi^* \subseteq \Psi = \{1, 2, \ldots, n_1\} \times \{1, 2, \ldots, n_2\}$$

Spatio-temporal process M denoted by $M_t(x)$ $(x \in \Psi, t \in \Upsilon)$.

$F_{s,t}(x, y)$ mass moving from location x at time s to y at time t.

Direct dependency of movement patterns F^0 and F^1:

Mass $F^0_{s,t}(x, y)$ positively associated with $F^1_{s,t}(x, y)$

(across all pairs of locations and times).

Use earth movers distance (EMD) (Kantorovich-Wasserstein metric).

Idea: Find minimal transportations costs

Earth mover's distance (EMD)

Non-negative spatial processes m^0 and m^1 over χ^0 and χ^1.

Work normalised by the total flow

$$\mathrm{EMD}(m^0, m^1) = \frac{\sum_{x \in \chi^0, y \in \chi^1} \hat{f}(x,y) d(x,y)}{\sum_{x \in \chi^0, y \in \chi^1} \hat{f}(x,y)}$$

Flow that minimises overall cost

$$\hat{f} = \mathrm{argmin}_{f \in \eta(m^0, m^1)} f(x,y) d(x,y),$$

for cost function $d(x,y)$ and $\eta(m^0, m^1)$ the set of f for which

$$f(x,y) \geq 0 \qquad \forall x \in \chi^0, y \in \chi^1$$

$$\sum_{x \in \chi^0} f(x,y) \leq m^1(y) \ \forall y \in \chi^1$$

$$\sum_{y \in \chi^1} f(x,y) \leq m^0(x) \ \forall x \in \chi^0$$

$$\sum_{x \in \chi^0, y \in \chi^1} f(x,y) = \min \left(\sum_{x \in \chi^0} m^0(x), \sum_{y \in \chi^1} m^1(y) \right).$$

Movement summary statistics

- Built on EMD
- Discretisation into 8 directions
- Subregions (to avoid unintuitive results from large spaces)
- Specification of Null hypothesis
- Permutation test set up
- Simulation study

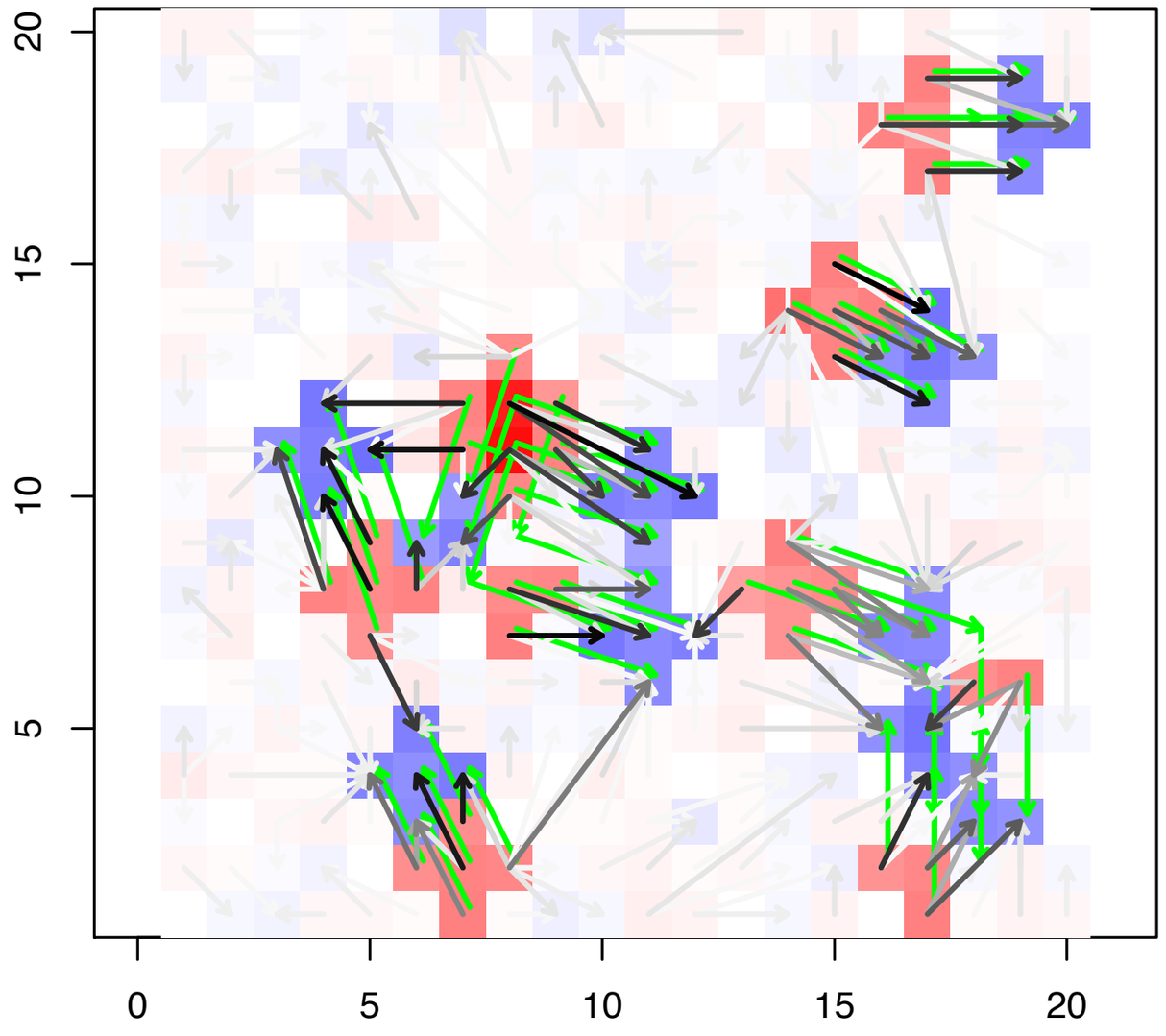

Null comprised of 3 statements

1. Between-sample independence of local bulk movement patterns:
   $\{S_{s,t}^{\psi_1,0}, S_{s,t}^{\psi_2,0}, \ldots, S_{s,t}^{\psi_w,0}\}$ independent of $\{S_{s,t}^{\psi_1,1}, S_{s,t}^{\psi_2,1}, \ldots, S_{s,t}^{\psi_w,1}\}$.

2. Specify set of operations Λ.

3. Within-sample independence of local bulk movement patterns:
   $S_{s,t}^{\psi_j}$ is independent of $S_{s,t}^{\psi_k}$ for $j \neq k$
   (required to ensure exchangeability under the action of $\lambda \in \Lambda$).

Example hypotheses

- Isotropic: rotation, reflection, reordering
- Homogeneous: reordering
- Symmetric: rotation, reflecting (limited)
- Horizontal reflection

Simulated data

Noise

$t = 1$ $t = 2$ $t = 3$ $t = 4$ $t = 5$

Isotropic

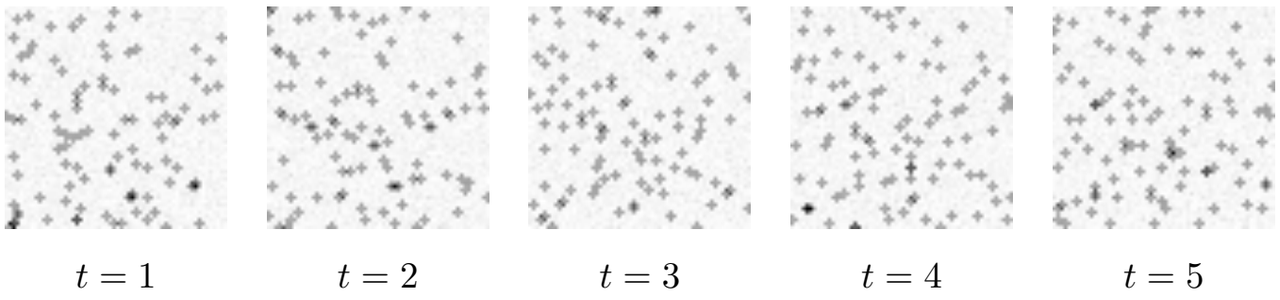

$t = 1$ $t = 2$ $t = 3$ $t = 4$ $t = 5$

Homogeneous

$t = 1$ $t = 2$ $t = 3$ $t = 4$ $t = 5$

Symmetric

$t = 1$ $t = 2$ $t = 3$ $t = 4$ $t = 5$

Simulation results

Independent movement

- mostly confirms theoretical method
- some issues with composite hypothesis

Dependent movement

- higher rate of incorrect rejections
- evidence for validity of omnibus hypothesis approach

Study II:
Evolution of bulk movement patterns

Question

Does the protein TACC3 evolve spatially colocalised with the protein EB3 during the process of mitosis?

Analysis

Compare movement patterns of TACC3 and EB3 during mitosis using EMD.

Results

Omnibus null hypothesis consistently rejected at 5%.

Conclusions

- Movement patterns of EB3 and TACC3 are dependent
- Potentially through their localisation on the tips of growing microtubules

Thanks

Microscopy work is joint with Tom Honnor (Warwick Statistics, now UCL), Adam Johnson (Warwick Statistics), Steve Royle (Warwick Medical School)

Thomas R. Honnor, Julia A. Brettschneider, Adam M. Johansen (2017),
Differences in spatial point patterns with application to subcellular biological structures

Honnor TR, Johansen AM and Brettschneider JA. (2017)
A nonparametric test for dependency between estimated local bulk movement patterns

Nixon, F.M., Honnor*, T.R., Starling, G.P., Beckett, A.J., Johansen, A.M., Brettschneider, J.A., Prior, I.A. & Royle, S.J.*
J Cell Science, April 2017
Microtubule organization within mitotic spindles revealed by serial block face scanning EM and image analysis